Deep Exclusive Reactions

Lecture 1: Nucleon structure studies with the electromagnetic probe
- Elastic scattering: form factors
- DIS: structure function
- Exclusive reactions: Generalized Parton Distributions

Lecture 2: Deeply Virtual Compton Scattering
- GPDs and DVCS
- DVCS on the proton with JLab@6 GeV
- Extraction of GPDs from data
- Proton tomography and forces in the proton

Lecture 3: DVCS and beyond
- DVMP
- New DVCS experiments@12 GeV
- TCS

Lecture 4: Perspectives
- Upgrades at JLab
- GPDs at the EIC

Lecture 5: Tutorial
- Data analysis techniques for exclusive reactions

CEBAF Large Acceptance Spectrometer

Silvia Niccolai, IJClab Orsay & CLAS Collaboration
PROBES Annual Meeting, Pisa (Italy), November 2025

Irène Joliot-Curie
Laboratoire de Physique des 2 Infinis

Multi-dimensional mapping of the nucleon

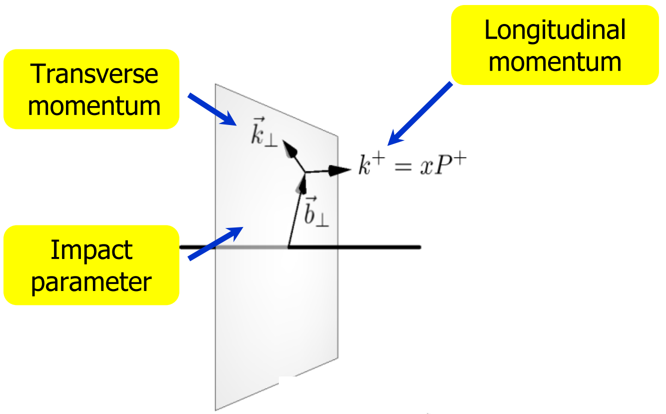

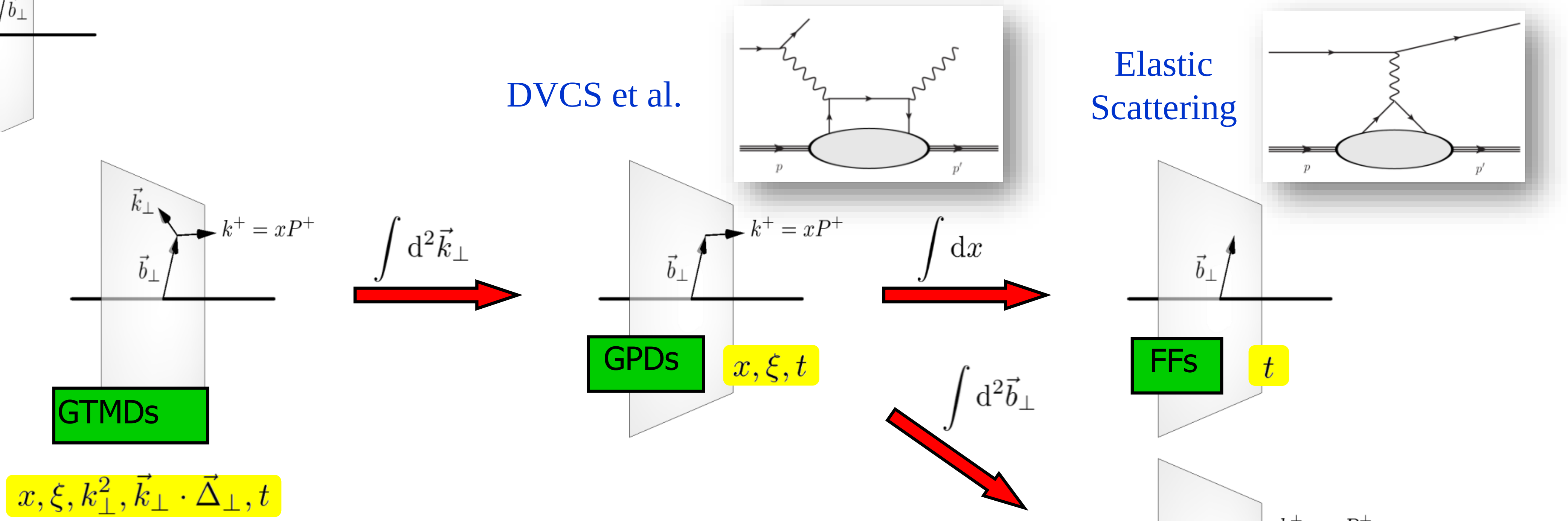

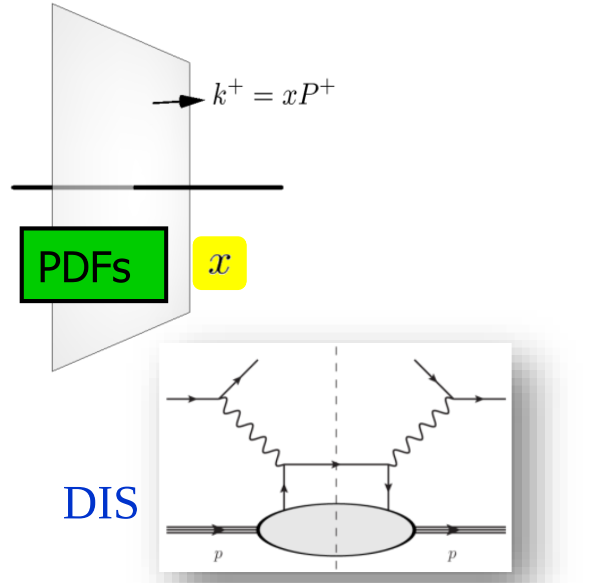

Operator in coordinate space	Nature of the matrix element	Associated structure functions in momentum space
$\langle p\vert\bar{\psi}(0)\mathcal{O}\psi(y)\vert p\rangle$	non-local, diagonal	$f_1(x), g_1(x)$
$\langle p'\vert\bar{\psi}(0)\mathcal{O}\psi(0)\vert p\rangle$	local, non-diagonal	$F_1(t), F_2(t), G_A(t), G_P(t)$
$\langle p'\vert\bar{\psi}(0)\mathcal{O}\psi(y)\vert p\rangle$	non-local, non-diagonal	$H(x,\xi,t), E(x,\xi,t), \tilde{H}(x,\xi,t), \tilde{E}(x,\xi,t)$

DVCS: the most direct road to access GPDs

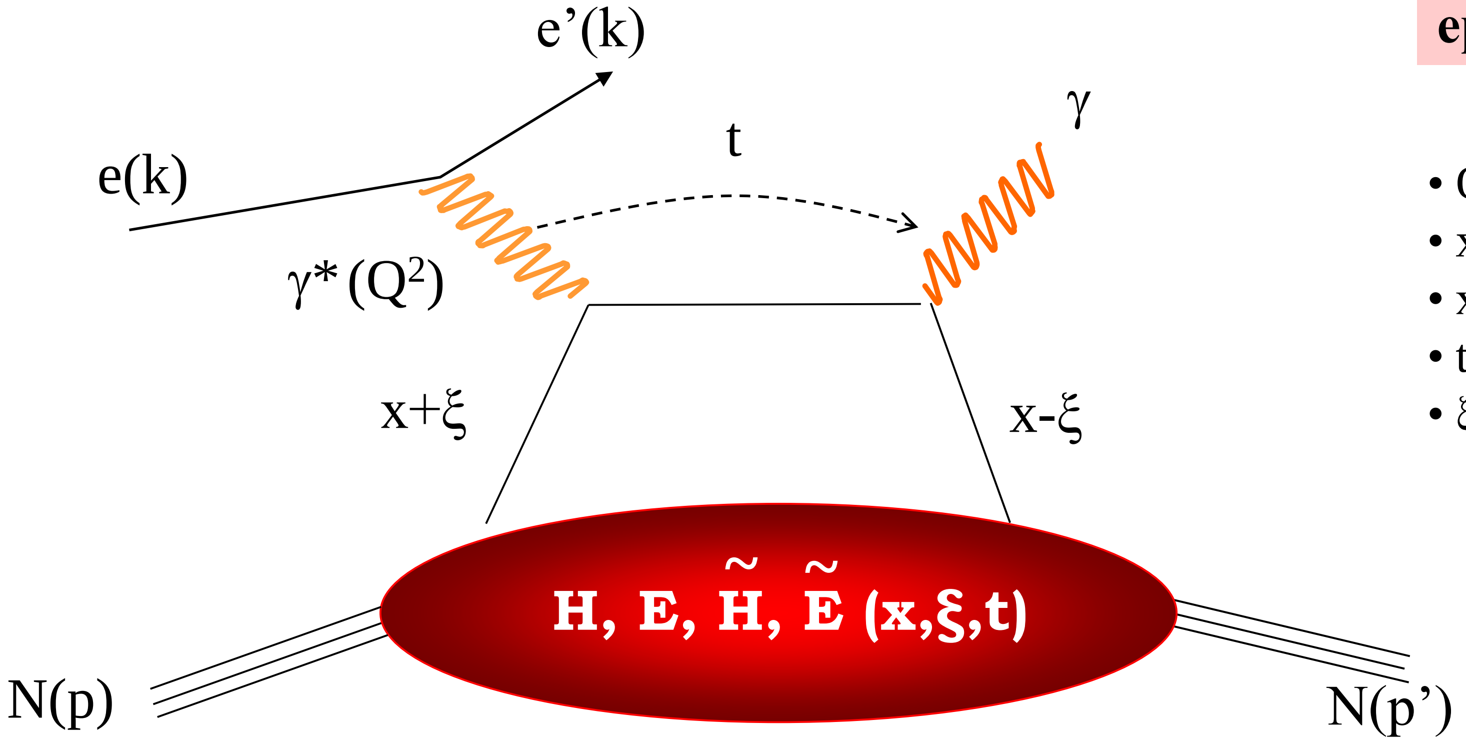

$ep \rightarrow e'p'\gamma$

- $Q^2 = -(k-k')^2$
- $x_B = Q^2/2M\nu \quad \nu = E_e - E_{e'}$
- $x+\xi$, $x-\xi$ longitudinal momentum fractions
- $t = \Delta^2 = (p-p')^2$
- $\xi \cong x_B/(2-x_B)$

DVCS and Bethe-Heitler: friends or enemies?

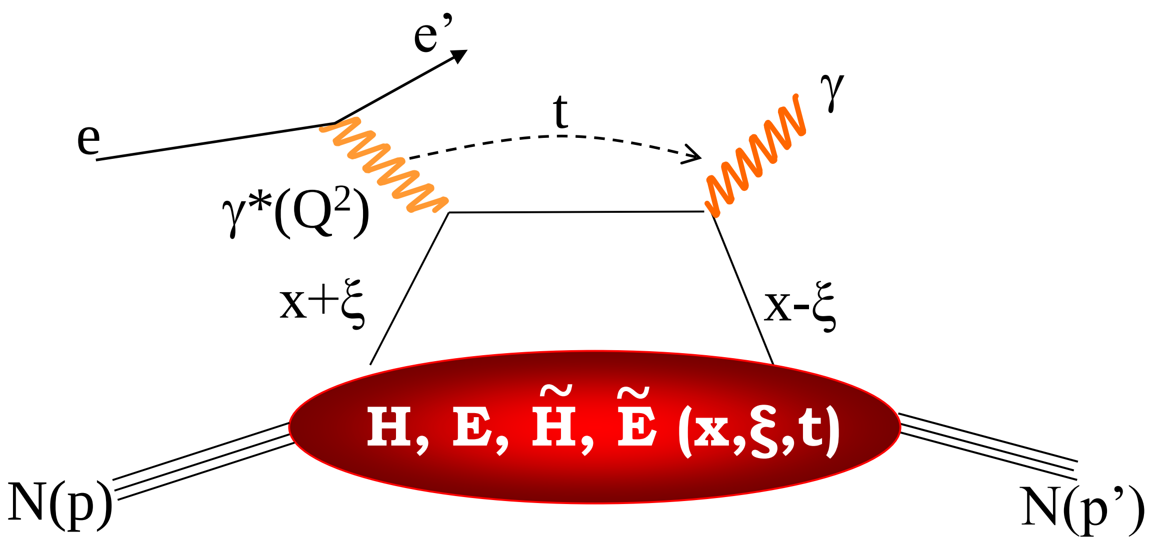

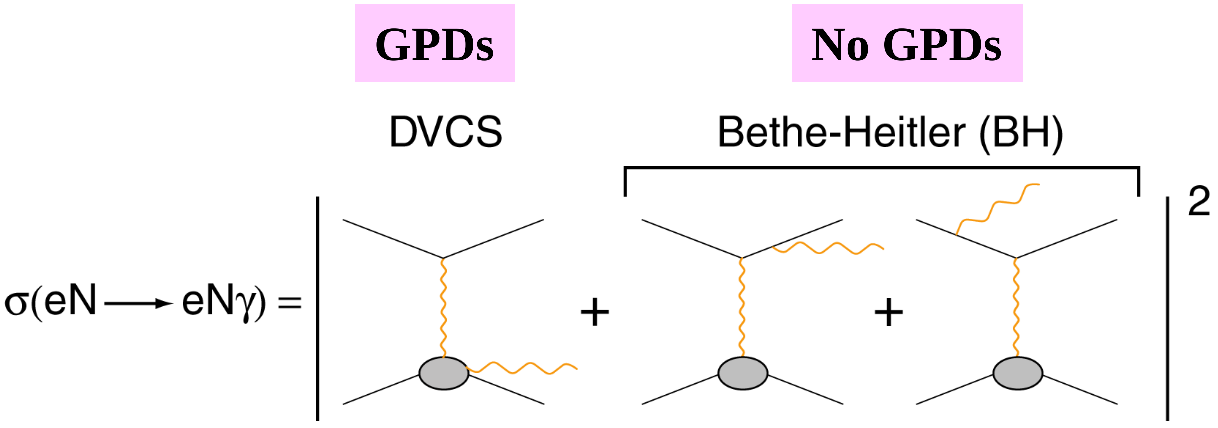

Calculable in QED thanks to our ~1% knowledge of form factors at low momentum transfer

$$|T|^2 = |T_{DVCS}|^2 + |T_{BH}|^2 + \underbrace{T_{DVCS}T^*_{BH} + T^*_{DVCS}T_{BH}}_{I}$$

$$\sigma(ep \to ep\gamma) = \underbrace{|BH|^2}_{\text{Known to} \sim 1\%} + \underbrace{\mathcal{I}(BH \cdot DVCS)}_{\text{Linear combination of GPDs}} + \underbrace{|DVCS|^2}_{\text{Bilinear combination of GPDs}}$$

In certains kinematics, the BH cross section dominates the DVCS one by orders of magnitude

DVCS and Bethe-Heitler: nucleon holography

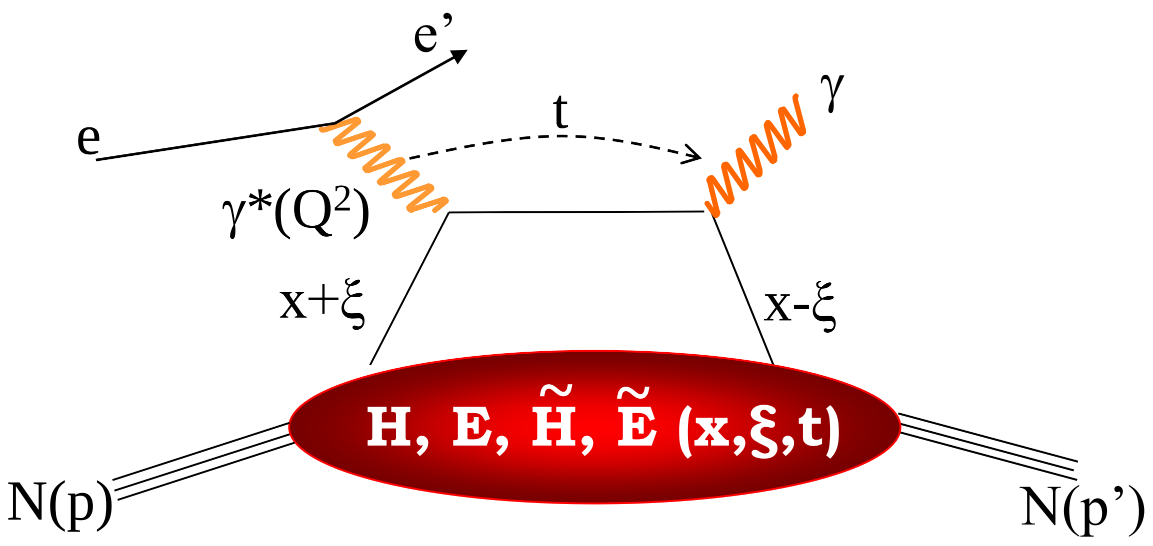

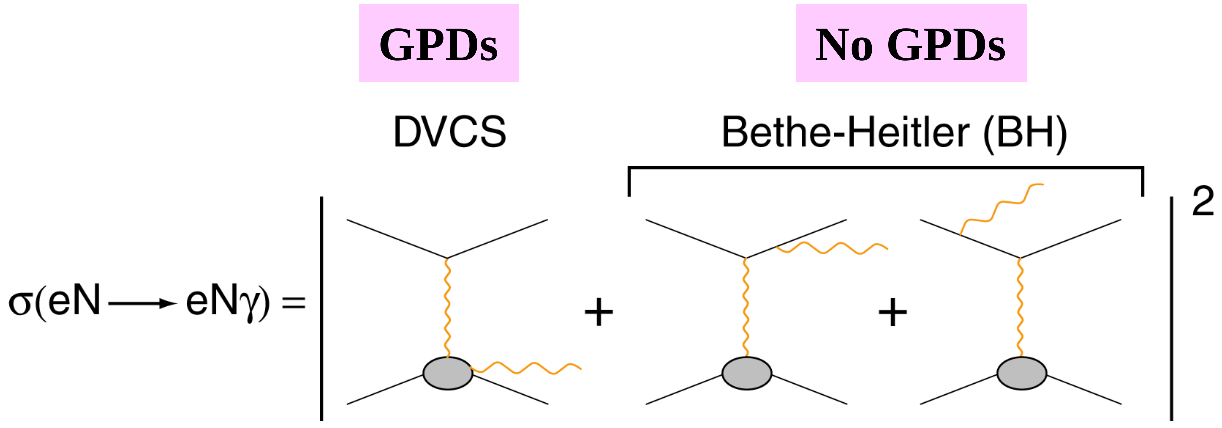

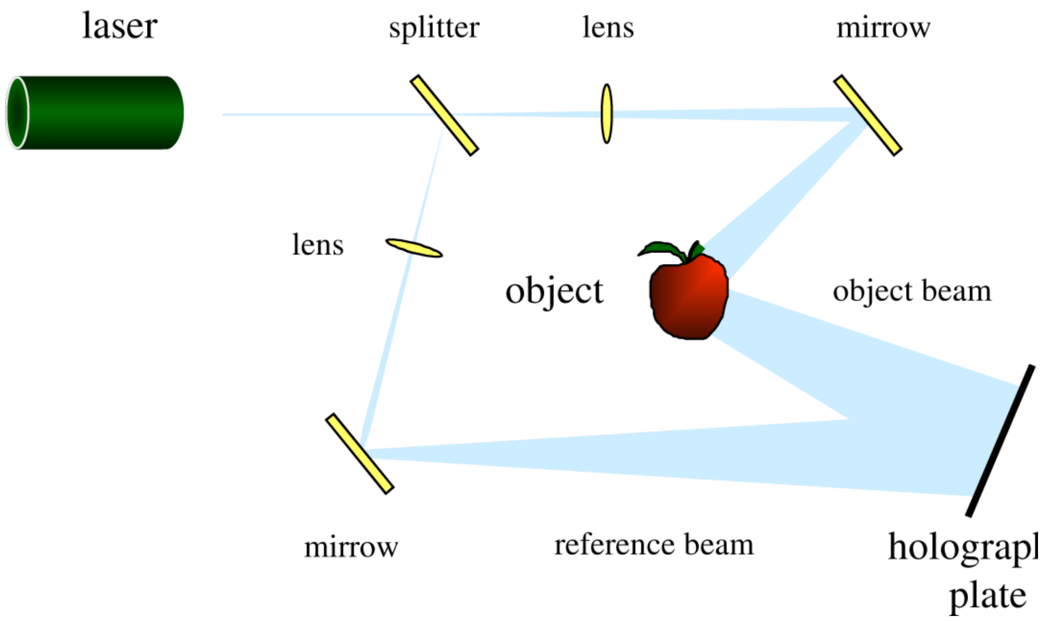

The interference of the reference light with the light reflected by the apple projects a 3 dimensional image of the apple on the screen

DVCS and Bethe-Heitler: nucleon holography

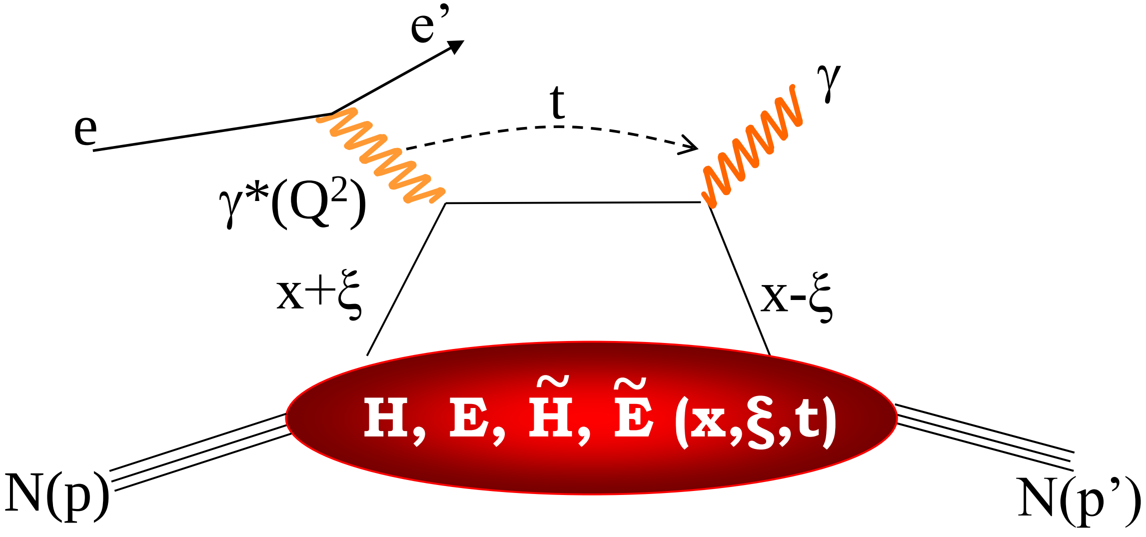

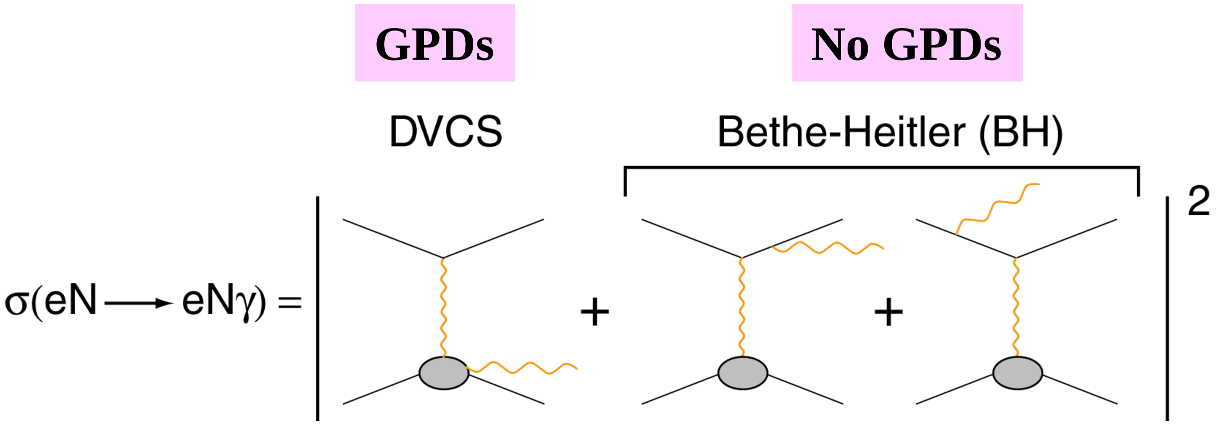

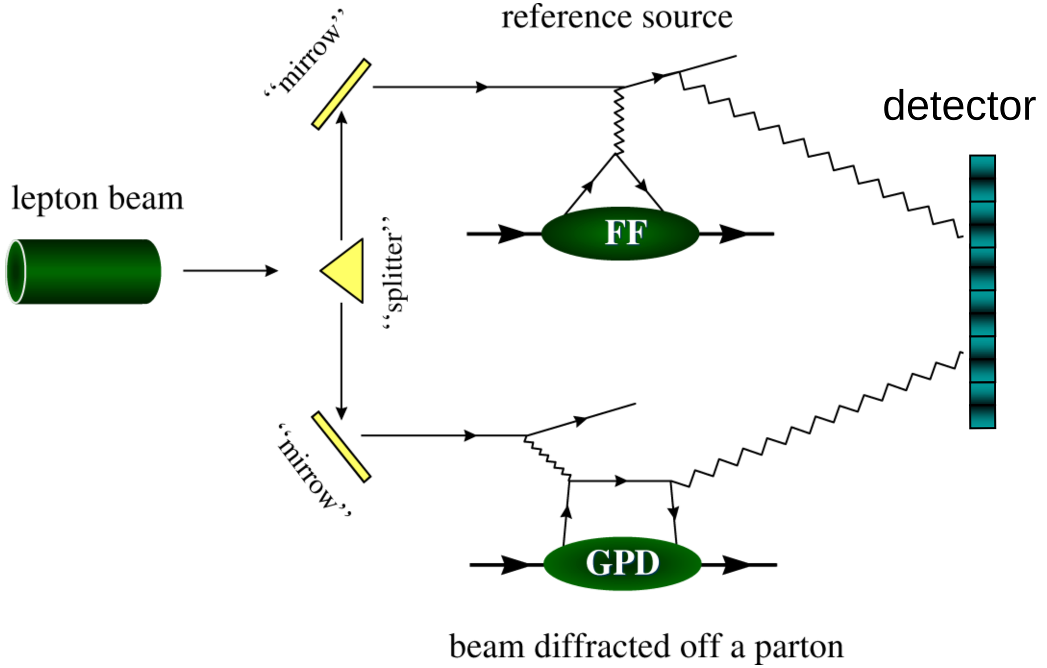

The interference of the Bethe Heitler and DVCS processes produces sizeable asymmetries that can be measured experimentally, giving access to GPDs

Accessing GPDs through DVCS

$$T^{DVCS} \sim \int_{-1}^{+1} \frac{GPD(x,\xi,t)}{x \pm \xi + i\varepsilon} dx + \ldots \sim P\int_{-1}^{+1} \frac{GPD(x,\xi,t)}{x \pm \xi} dx \pm i\pi GPD(\pm\xi,\xi,t) + \ldots$$

$$\boxed{Re\mathcal{H}_q = e_q^2 P\int_0^{+1} \left(H^q(x,\xi,t) - H^q(-x,\xi,t)\right)\left[\frac{1}{\xi - x} + \frac{1}{\xi + x}\right] dx}$$

$$Im\mathcal{H}_q = \pi e_q^2 \left[H^q(\xi,\xi,t) - H^q(-\xi,\xi,t)\right]$$

Real and imaginary parts of **Compton Form Factors**

Only ξ and t are accessible experimentally by DVCS

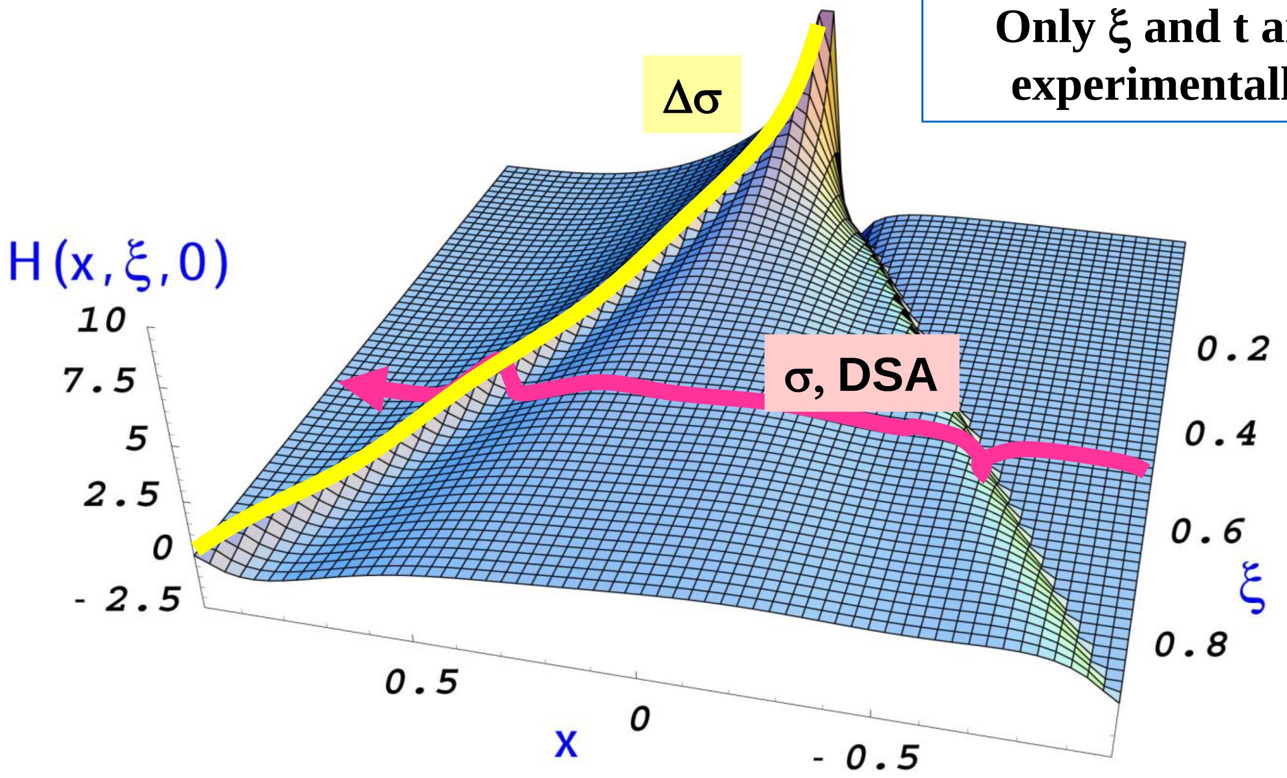

$$\sigma \sim |T^{DVCS} + T^{BH}|^2$$

$$\Delta\sigma = \sigma^+ - \sigma^- \propto I(DVCS \cdot BH)$$

$$A = \frac{\Delta\sigma}{\sigma^+ + \sigma^-} \propto \frac{I(DVCS \cdot BH)}{|BH|^2 + |DVCS|^2 + I}$$

Azimuthal dependence of the ep→epγ cross section

$$\frac{d^5\sigma}{dQ^2 dx_B d\varphi_e dt d\varphi} = \frac{\alpha^3 x_B y}{16\pi^2 Q^2 \sqrt{1+4x_B^2 M^2/Q^2}} \left| \frac{\mathcal{T}}{e^3} \right|^2$$

$$|\mathcal{T}|^2 = |\mathcal{T}_{\rm BH}|^2 + |\mathcal{T}_{\rm DVCS}|^2 + \mathcal{I}$$

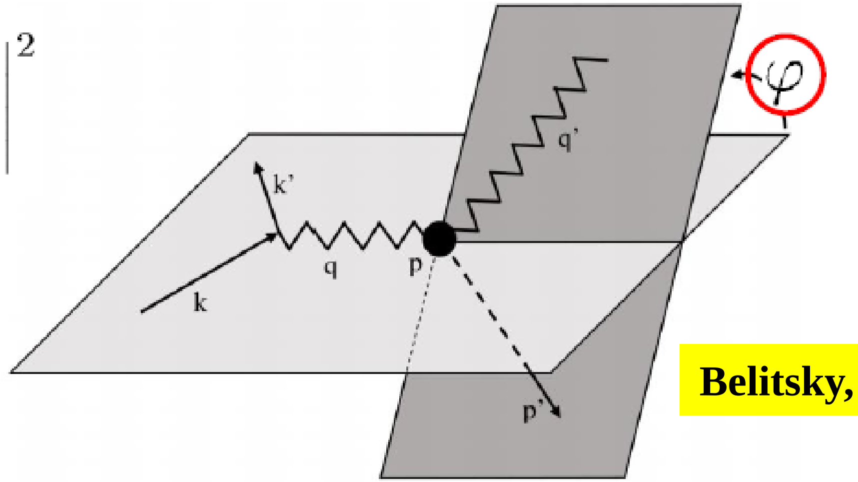

Belitsky, Müller, Kirchner (2000)

$$|\mathcal{T}_{\rm BH}|^2 = \frac{e^6}{x_B^2 y^2 [1+4x_B^2 M^2/Q^2]^2 t \mathcal{P}_1(\varphi)\mathcal{P}_2(\varphi)} \left\{ c_0^{\rm BH} + \sum_{n=1}^{2} c_n^{\rm BH} \cos(n\varphi) + s_1^{\rm BH} \sin\varphi \right\},$$

$$|\mathcal{T}_{\rm DVCS}|^2 = \frac{e^6}{y^2 Q^2} \left\{ c_0^{\rm DVCS} + \sum_{n=1}^{2} \left[c_n^{\rm DVCS} \cos(n\varphi) + s_n^{\rm DVCS} \sin(n\varphi) \right] \right\},$$

$$\mathcal{I} = \frac{\pm e^6}{x_B y^3 t \mathcal{P}_1(\varphi)\mathcal{P}_2(\varphi)} \left\{ c_0^{\mathcal{I}} + \sum_{n=1}^{3} \left[c_n^{\mathcal{I}} \cos(n\varphi) + s_n^{\mathcal{I}} \sin(n\varphi) \right] \right\},$$

Accessing GPDs through DVCS polarization observables

Proton Neutron

Polarized beam, unpolarized target:

$\Delta\sigma_{LU} \sim \sin\phi \; \mathrm{Im}\{F_1\mathcal{H} + \xi(F_1+F_2)\tilde{\mathcal{H}} - kF_2\mathcal{E} + \ldots\}$ $\Rightarrow$ $Im\{\mathcal{H}_p, \tilde{\mathcal{H}}_p, \mathcal{E}_p\}$ $Im\{\mathcal{H}_n, \tilde{\mathcal{H}}_n, \mathcal{E}_n\}$

Unpolarized beam, longitudinal target:

$\Delta\sigma_{UL} \sim \sin\phi \mathrm{Im}\{F_1\tilde{\mathcal{H}} + \xi(F_1+F_2)(\mathcal{H} + x_B/2\mathcal{E}) - \xi kF_2\tilde{\mathcal{E}}\}$ $\Rightarrow$ $Im\{\mathcal{H}_p, \tilde{\mathcal{H}}_p\}$ $Im\{\mathcal{H}_n, \mathcal{E}_n\}$

Polarized beam, longitudinal target:

$\Delta\sigma_{LL} \sim (A+B\cos\phi)\mathrm{Re}\{F_1\tilde{\mathcal{H}} + \xi(F_1+F_2)(\mathcal{H} + x_B/2\mathcal{E}) + \ldots\}$ $\Rightarrow$ $Re\{\mathcal{H}_p, \tilde{\mathcal{H}}_p\}$ $Re\{\mathcal{H}_n, \mathcal{E}_n\}$

Unpolarized beam, transverse target:

$\Delta\sigma_{UT} \sim \cos\phi \sin(\phi_s - \phi)\mathrm{Im}\{k(F_2\mathcal{H} - F_1\mathcal{E}) + \ldots\}$ $\Rightarrow$ $Im\{\mathcal{H}_p, \mathcal{E}_p\}$ $Im\{\mathcal{H}_n\}$

Unpolarized beam and target, different lepton charges:

$\Delta\sigma_C \sim \cos\phi \; \mathrm{Re}\{F_1\mathcal{H} + \xi(F_1+F_2)\tilde{\mathcal{H}} - kF_2\mathcal{E} + \ldots\}$ $\Rightarrow$ $Re\{\mathcal{H}_p, \tilde{\mathcal{H}}_p, \mathcal{E}_p\}$ $Re\{\mathcal{H}_n, \tilde{\mathcal{H}}_n, \mathcal{E}_n\}$

$$\sigma \sim |T^{DVCS} + T^{BH}|^2$$

$$\Delta\sigma = \sigma^+ - \sigma^- \propto I(DVCS \cdot BH)$$

$$A = \frac{\Delta\sigma}{\sigma^+ + \sigma^-} \propto \frac{I(DVCS \cdot BH)}{|BH|^2 + |DVCS|^2 + I}$$

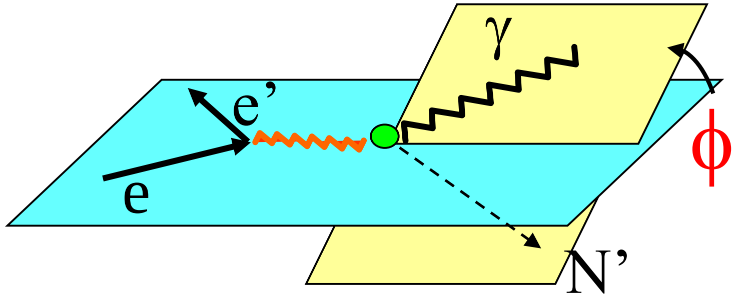

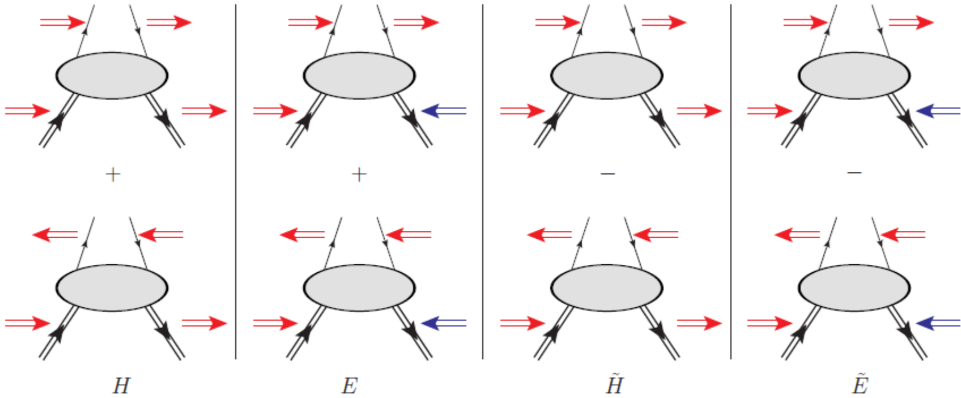

GPDs through DVCS: experimental and theoretical challenges

- GPDs can offer insights in many aspects of nucleon structure: nucleon tomography, partons' angular momentum, distribution of forces in the nucleon
- At the highest level of approximation, there are 4 GPDs for each quark flavor that need to be constrained
- Each GPD depends on 3 kinematic variables
- DVCS allows access to CFF, which depend only on 2 of those 3 kinematic variables
- DVCS interferes with BH, mixed blessing: BH dominates the cross section, interference depends linearly on CFFs and is accessed in polarization asymmetries
- DVCS is an exclusive final state with a small cross section: high intensity lepton beam and high luminosity are needed
- Polarization observables are needed to single out the contributions of the various GPDs: polarized beams and targets
- Wide phase-space coverage is needed to sample the rich kinematic dependence of the GPDs

→ **Jefferson Lab is the ideal facility for DVCS measurements**

DVCS experiments worldwide

DESY	
HERMES	***H1/ZEUS***
p-DVCS BSA,BCA, tTSA,lTSA,DSA	p-DVCS X-sec,BCA

CERN
COMPASS
p-DVCS X-sec,BSA,BCA, tTSA,lTSA,DSA

JLAB	
Hall A	***Hall B***
p,n-DVCS (Bpol.) X-sec	p-DVCS BSA,lTSA,DSA,X-sec

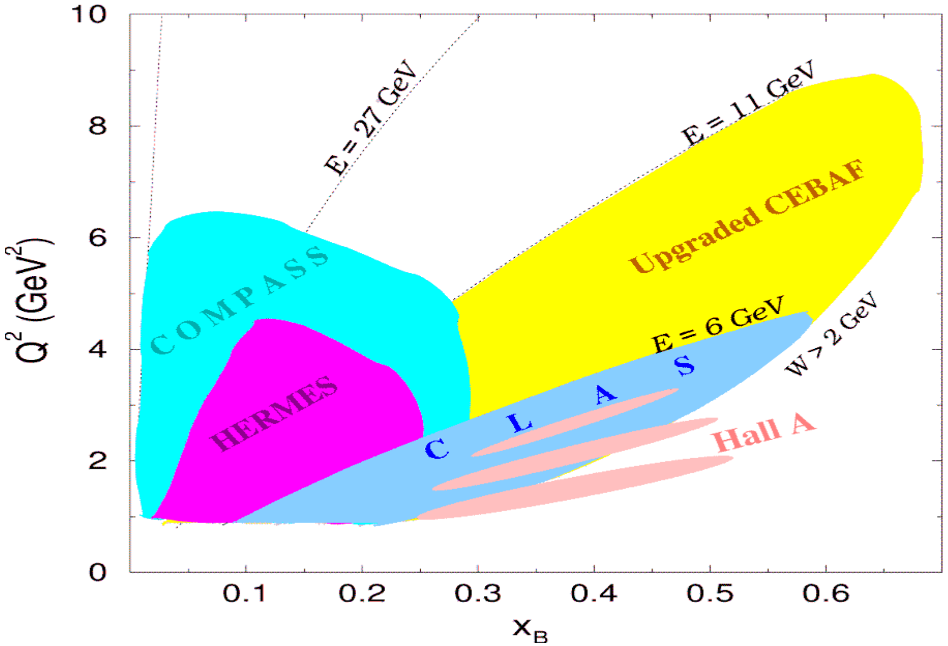

JLab@6 GeV

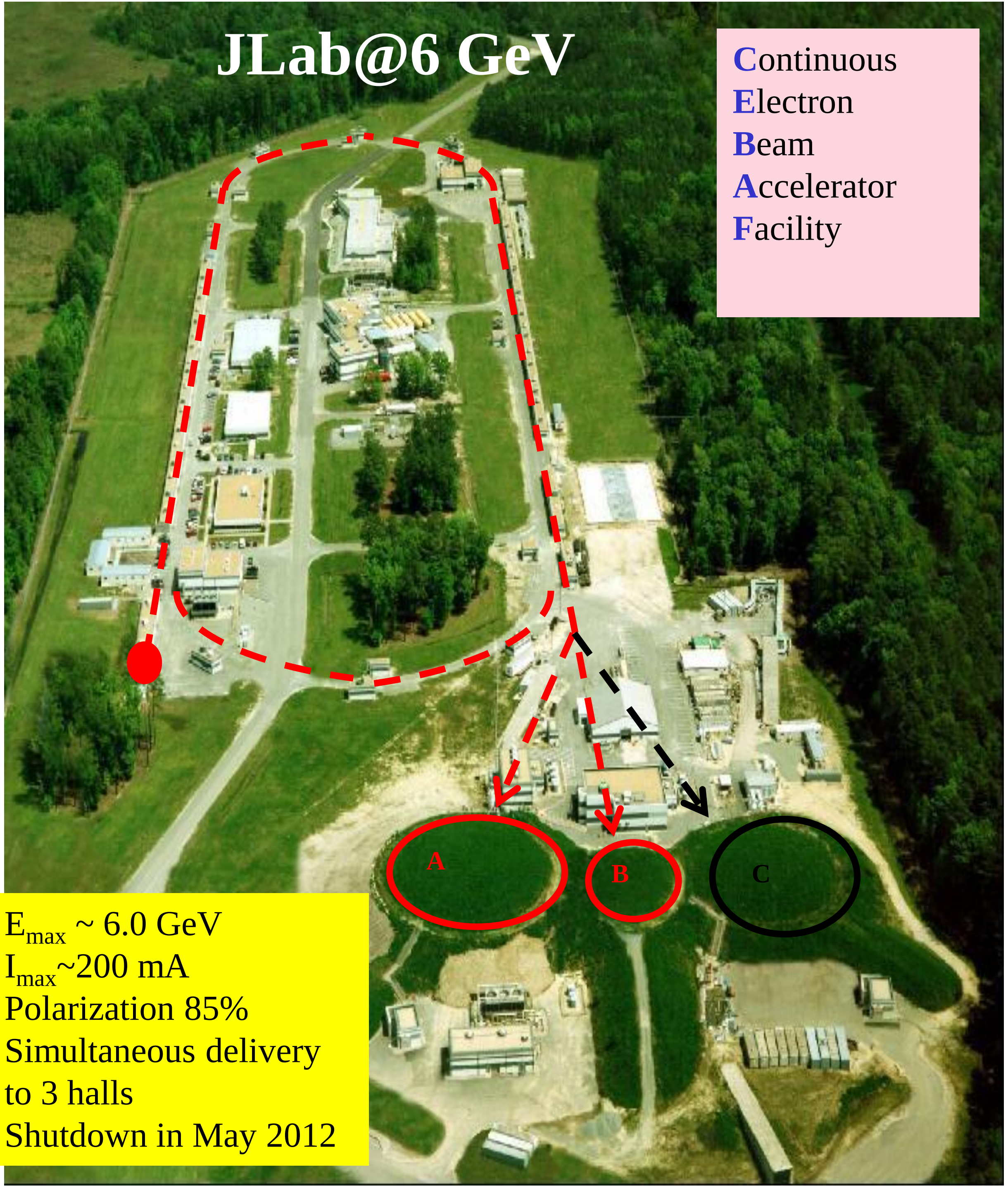

Continuous
Electron
Beam
Accelerator
Facility

- E_{max} ~ 6.0 GeV
- I_{max}~200 mA
- Polarization 85%
- Simultaneous delivery to 3 halls
- Shutdown in May 2012

Hall A: 2 HRS
High resolution
High luminosity ($L\sim10^{37}$)
Limited coverage

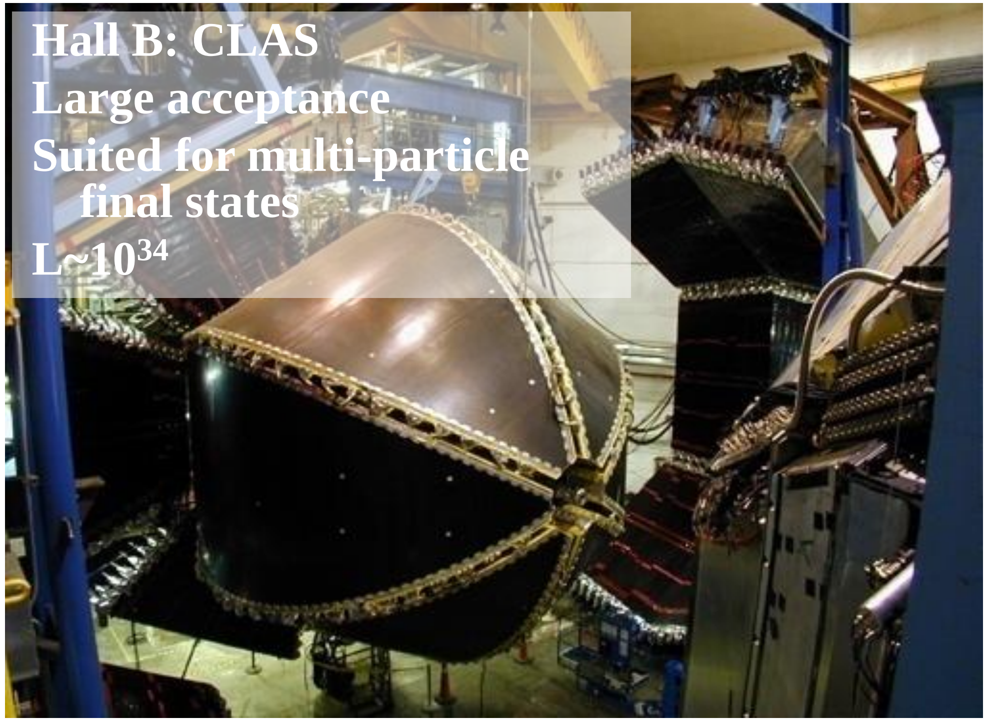

Hall B: CLAS
Large acceptance
Suited for multi-particle final states
$L\sim10^{34}$

DVCS @ CLAS and HERMES: first pioneering results

NON-DEDICATED experiments

ep→epX

S. Stepanyan et al., PRL 87 (2001)

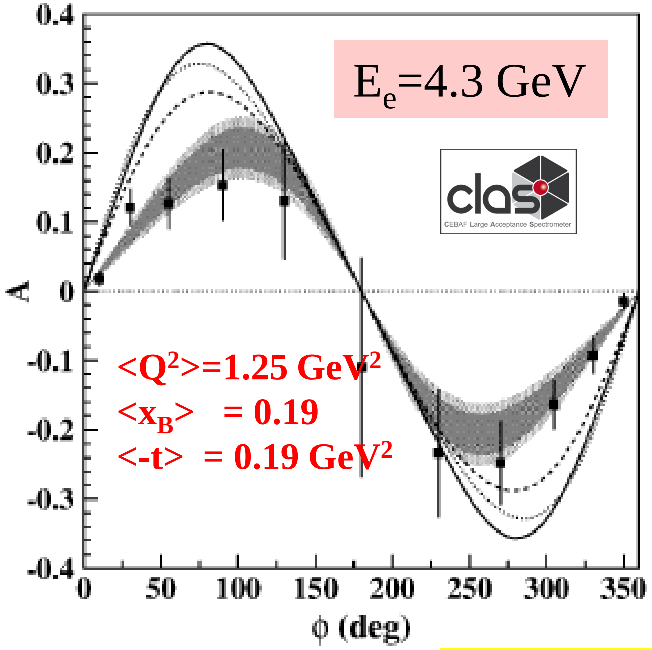

ep→eγX

A. Airapetian et al., PRL 87 (2001)

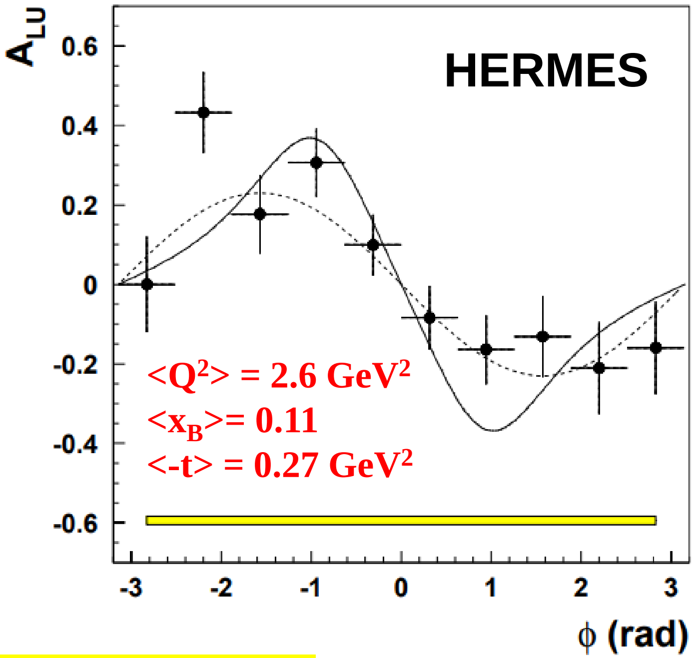

ep→epγ

S. Chen et al., PRL 97 (2006)

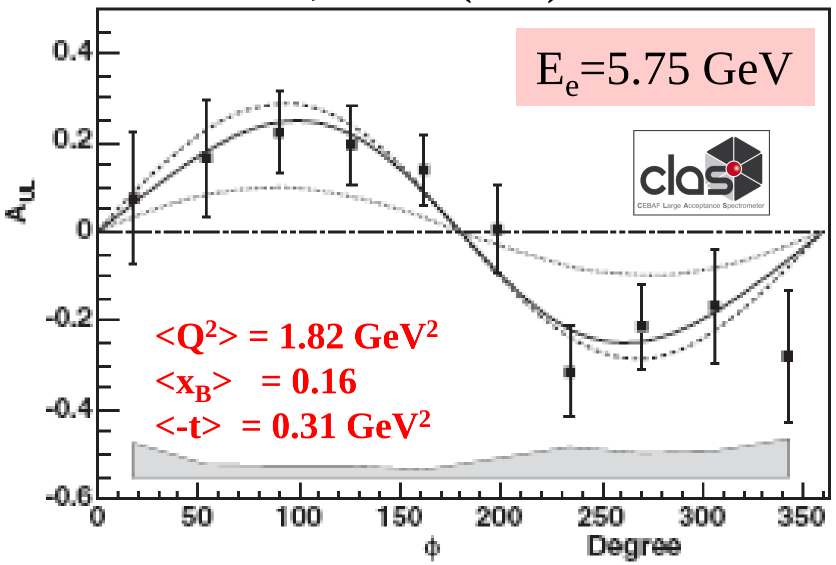

BSA ~ $Im\{\mathcal{H}_p, \tilde{\mathcal{H}}_p, \mathcal{E}_p\}$

TSA ~ $Im\{\mathcal{H}_p, \tilde{\mathcal{H}}_p\}$

$A(\phi) = \alpha\sin\phi + \beta\sin2\phi$

$\beta/\alpha \ll 1$ → twist-2 (handbag) dominance

BSA, BCA and TSA (T & L) at HERMES: handbag dominance confirmed

- ✓ Low statistics
- ✓ Integrated over all kinematics
- ✓ Uncertainties on determination of epγ final state

Hall A (JLab): first dedicated DVCS experiment

ep→eγX

Polarized cross section difference

C.M. Camacho et al., PRL 97 (2006)

Q² evolution→ evidence for scaling

(small Q² range)

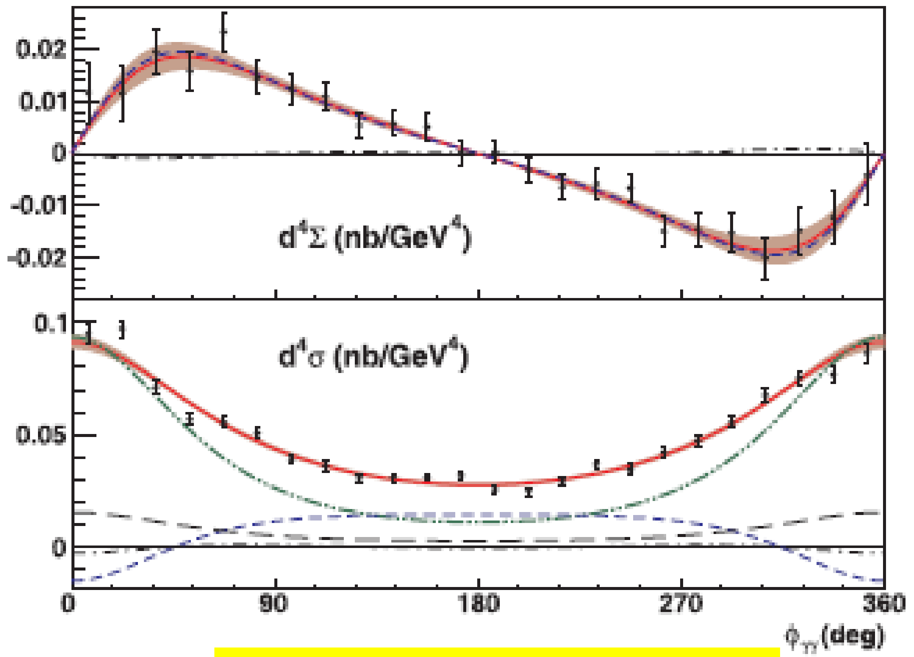

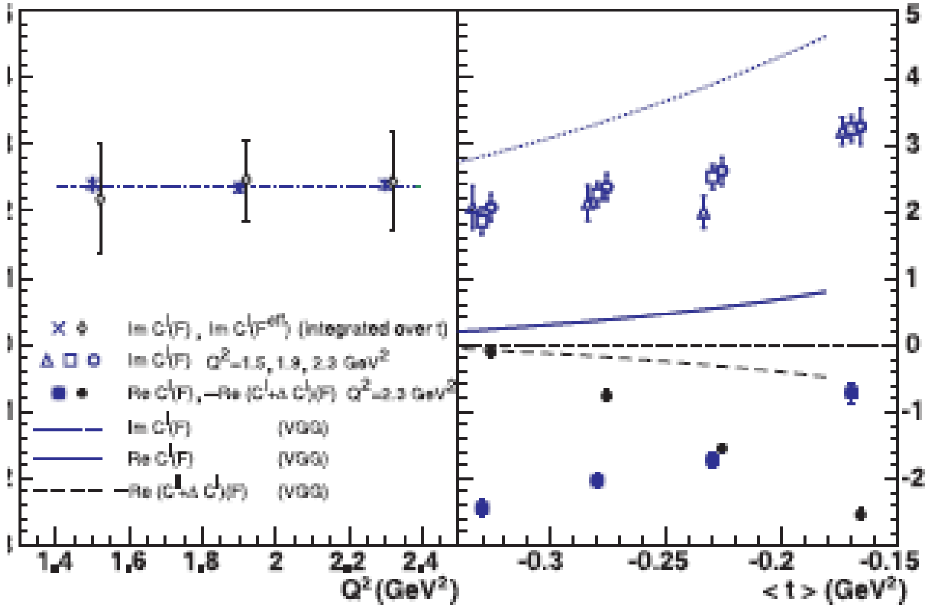

Unpolarized cross section

<Q2, -t> = (2.3,-0.28)

Formalism of Belitsky, Mueller, Kirchner

Fit

$|BH|^2$

Inteference BH-DVCS

High resolution→exclusivity
High luminosity→precision
Limited phase space

The CLAS e1-DVCS experiment

Data taken in the spring **2005**
- Beam energy ~ **5.75 GeV**
- Beam polarization ~ **80%**
- Target **LH_2**

Added to the standard CLAS
✓ Solenoid magnet +
✓ **IC (inner calorimeter):**
424 lead-tungstate crystals
+ APD readout

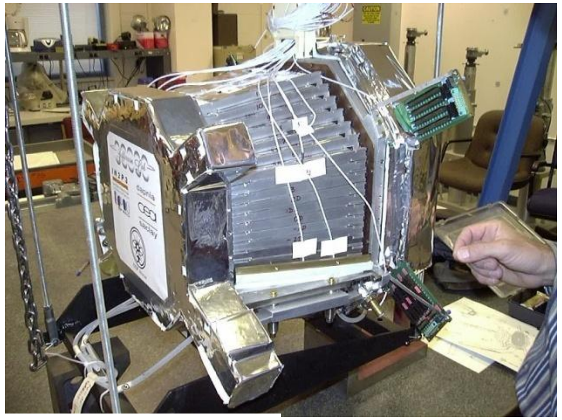

BSA ~ $Im\{\mathcal{H}_p, \widetilde{\mathcal{H}}_p, \mathcal{E}_p\}$

$\vec{e}p \rightarrow ep\gamma$

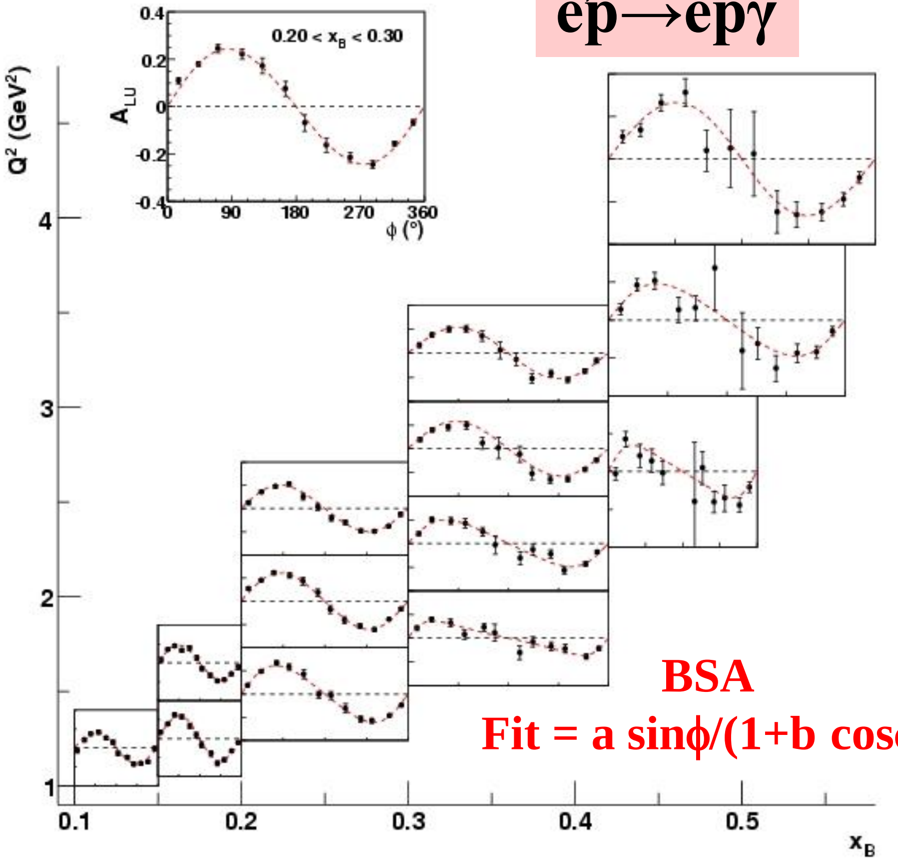

BSA
Fit = a sinϕ/(1+b cosϕ)

F.X. Girod et al., PRL 100 (2008)

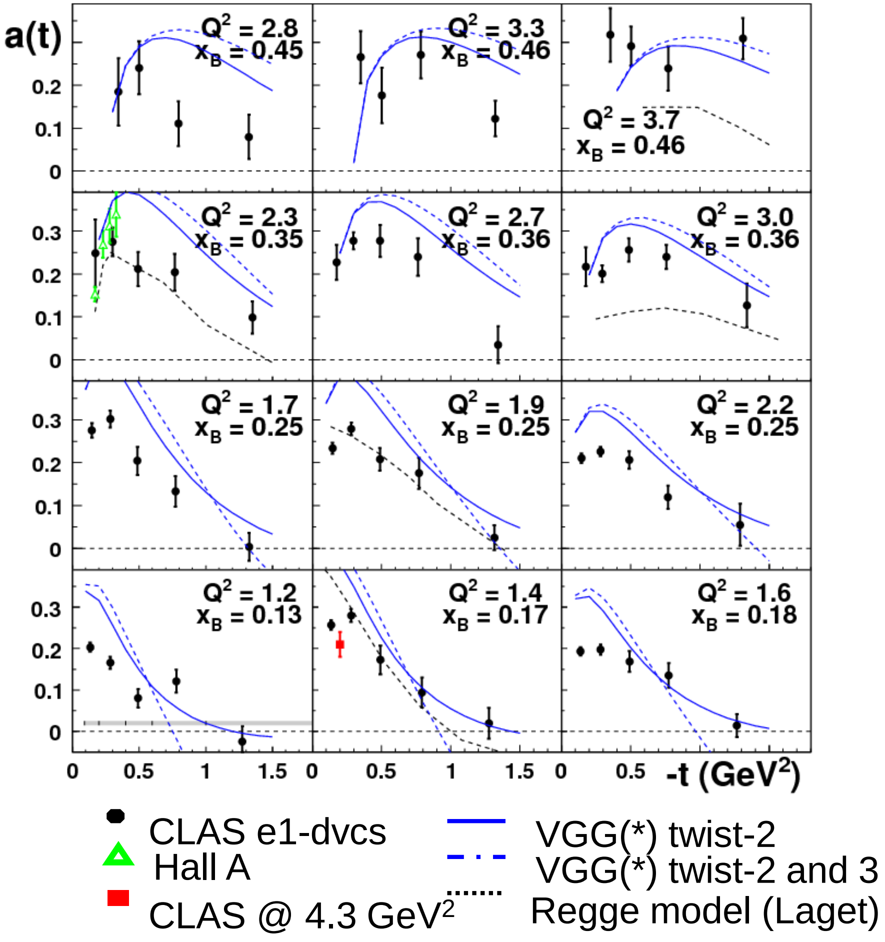

(*) Vanderhaegen, Guichon, Guidal

CLAS: unpolarized and beam-polarized cross sections

$\vec{e}p \rightarrow ep\gamma$

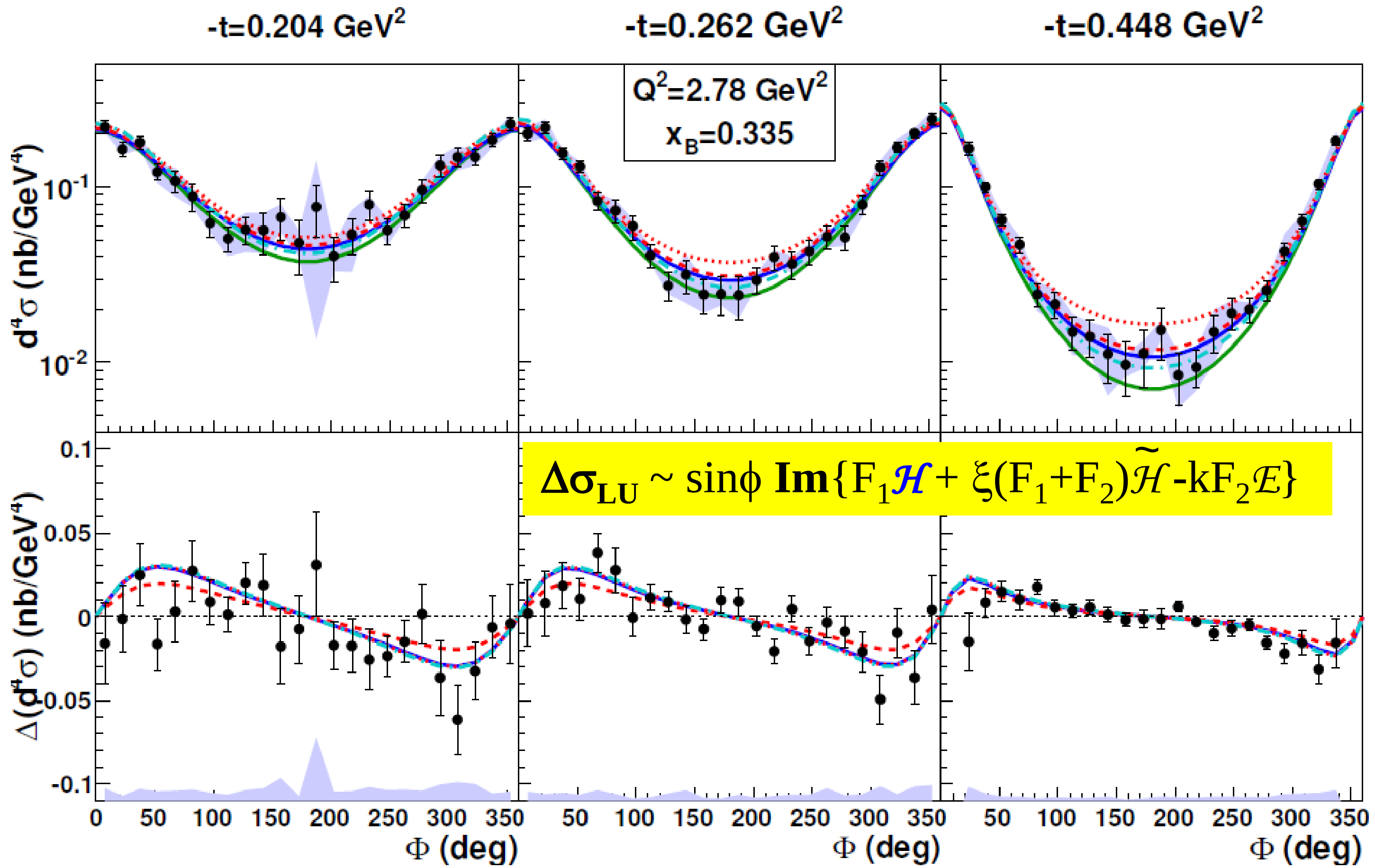

H.S. Jo et al., PRL 115 (2015)

- Beam energy ~ **5.75 GeV**
- Beam polarization ~ **80%**
- Target $\mathbf{LH_2}$
- CLAS+Inner Calorimeter

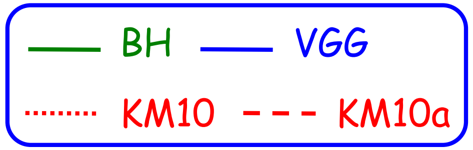

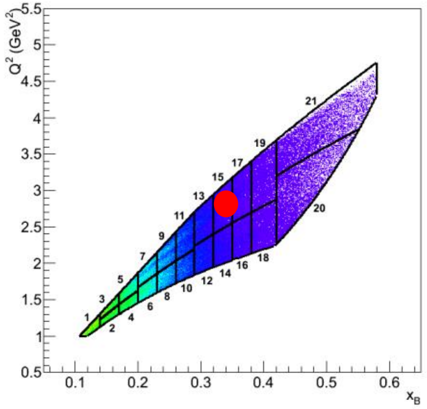

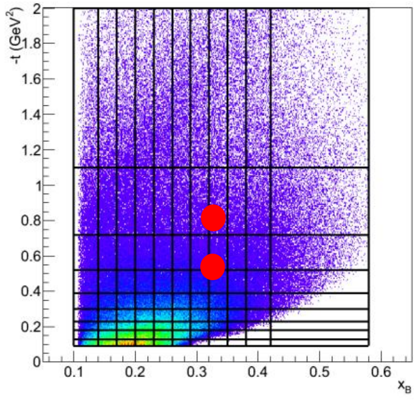

- **Two observables extracted**
- **Largest kinematics ever covered for DVCS**

21 Q^2-x_B bins, 9 t bins, 24 φ bins

CLAS: DVCS on longitudinally polarized target

- Beam energy **~5.9 GeV**
- CLAS + IC to detect forward photons
- Target: **longitudinally polarized NH_3** (P~80%)
- **3 DVCS observables**

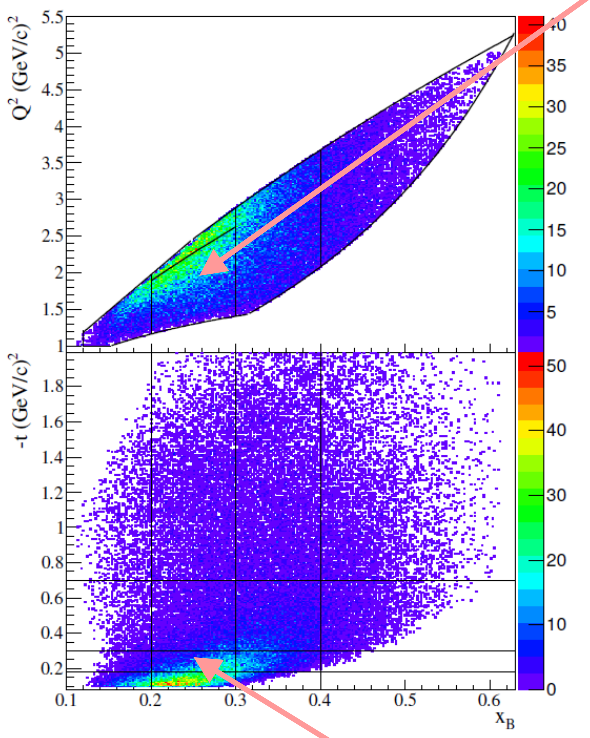

- **5 Q^2-x_B bins**
- **4 t bins**
- **10 ϕ bins**

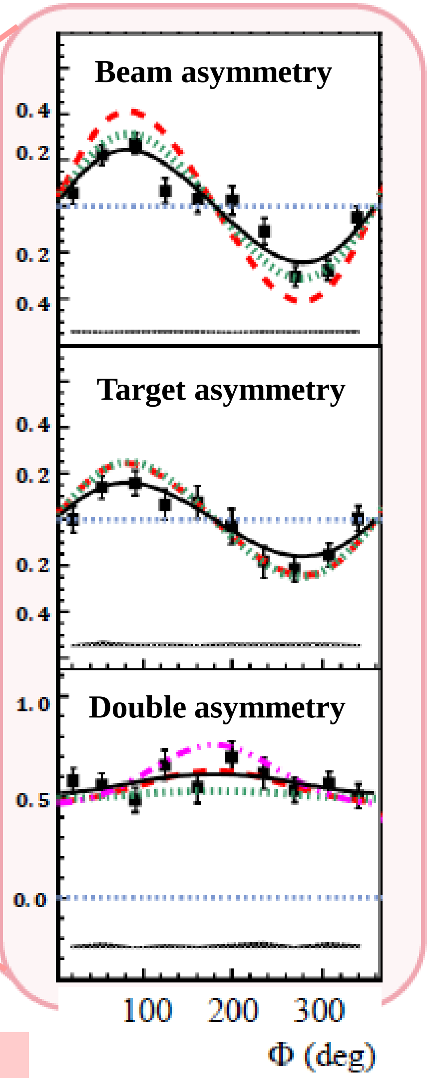

E. Seder et al., PRL 114 (2015)

S. Pisano et al., PRD 91 (2015)

TSA ~ $Im\{\tilde{\mathcal{H}}_p, \mathcal{H}_p\}$

$\vec{e}\vec{p} \rightarrow ep\gamma$

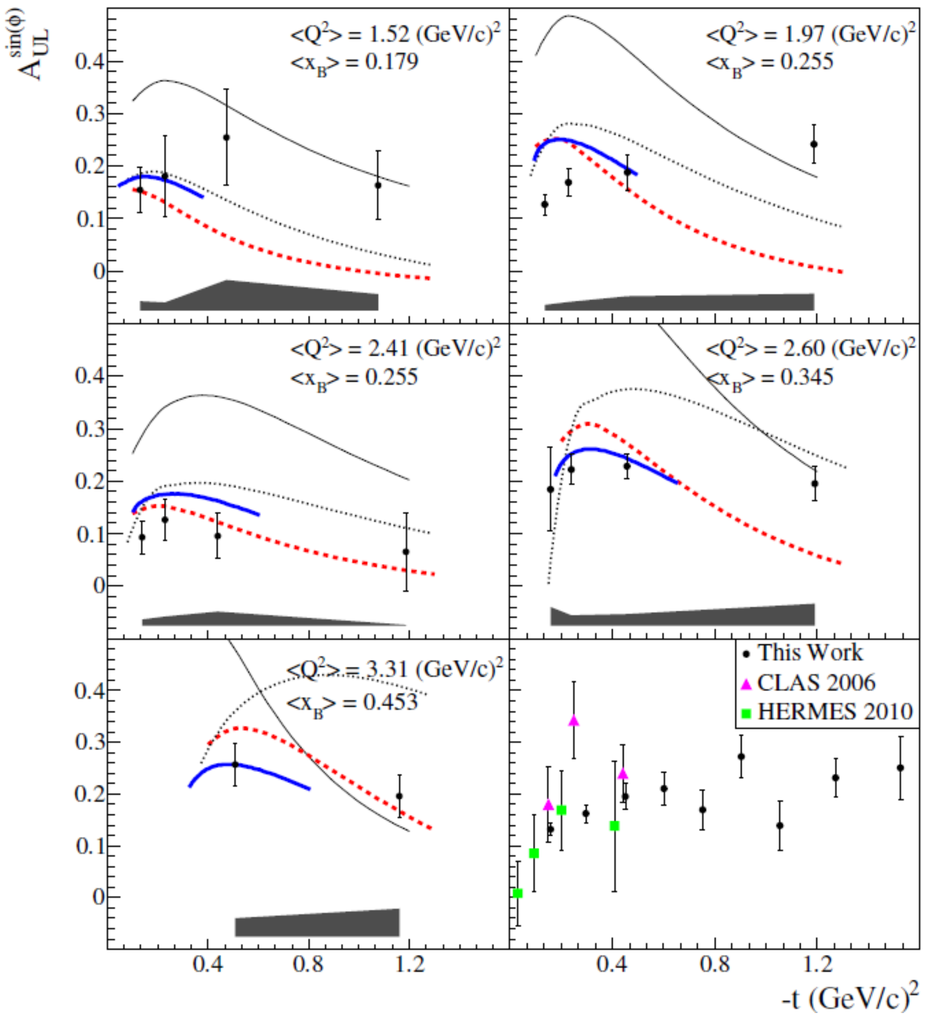

- **Improved statistics x10 at low –t**
- **Extended kinematic coverage**

Extraction of Compton Form Factors from DVCS observables

Various possible techniques/strategies:

- Local fits: each kinematic bin is treated independently. Each CFF (*Im*$\mathcal{H}$, *Re*$\mathcal{H}$, *Im*$\mathcal{E}$…) is a free fit parameter (M. Guidal)
- Global fits: all kinematic bins are taken at the same time. Parametrizations of the GPDs or CFFs are used (G. Goldstein et al., K. Kumericki and D. Mueller)
- Hybrid local/global fits: combination of the two methods above, that allows to estimate systematic uncertainties (H. Moutarde)
- Neural networks: already extensively used for PDF fits. Recently started for GPDs (K. Kumericki)

8 CFF

$$
\left\{
\begin{aligned}
\mathrm{Re}(\mathcal{H}) &= P\int_0^1 dx\left[H(x,\xi,t) - H(-x,\xi,t)\right]C^+(x,\xi)\\
\mathrm{Re}(\mathcal{E}) &= P\int_0^1 dx\left[E(x,\xi,t) - E(-x,\xi,t)\right]C^+(x,\xi)\\
\mathrm{Re}(\tilde{\mathcal{H}}) &= P\int_0^1 dx\left[\tilde{H}(x,\xi,t) + \tilde{H}(-x,\xi,t)\right]C^-(x,\xi)\\
\mathrm{Re}(\tilde{\mathcal{E}}) &= P\int_0^1 dx\left[\tilde{E}(x,\xi,t) + \tilde{E}(-x,\xi,t)\right]C^-(x,\xi)\\
\mathrm{Im}(\mathcal{H}) &= H(\xi,\xi,t) - H(-\xi,\xi,t)\\
\mathrm{Im}(\mathcal{E}) &= E(\xi,\xi,t) - E(-\xi,\xi,t)\\
\mathrm{Im}(\tilde{\mathcal{H}}) &= \tilde{H}(\xi,\xi,t) - \tilde{H}(-\xi,\xi,t)\\
\mathrm{Im}(\tilde{\mathcal{E}}) &= \tilde{E}(\xi,\xi,t) - \tilde{E}(-\xi,\xi,t)
\end{aligned}
\right.
$$

$$
\text{with } C^{\pm}(x,\xi) = \frac{1}{x-\xi} \pm \frac{1}{x+\xi}
$$

M. Guidal: **Model-independent fit**, at fixed Q^2, x_B and t of DVCS observables; 8 unknowns (the CFFs), non-linear problem, strong correlations. Bounding the domain of variation of the CFFs with model (5xVGG)
M. Guidal, Eur. Phys. J. A 37 (2008), and other articles

Results for H_{Im} and $\tilde{H}_{Im}$ from the fits of JLab 2015 data

CFFs fitting code by M. Guidal

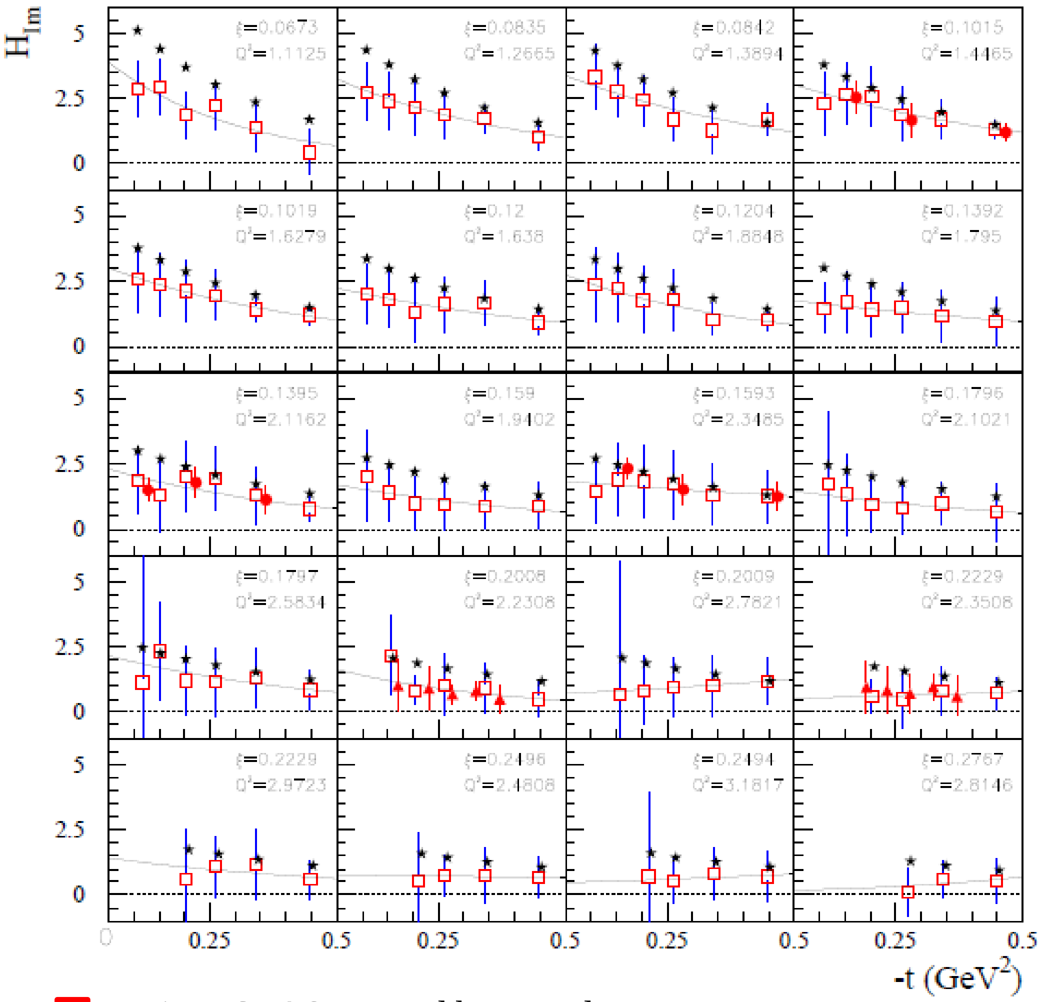

- Fit to CLAS c.s. and beam pol. c.s.
- Fit to CLAS c.s., beam pol. c.s., lTSA, DSA
- Fit to Hall A c.s. and beam pol. c.s.
- VGG model

***Im$\mathcal{H}$*, flatter t slope at high x_B: faster quarks (valence) at the core of the proton, slower quarks (sea) at its periphery → PROTON TOMOGRAPHY**

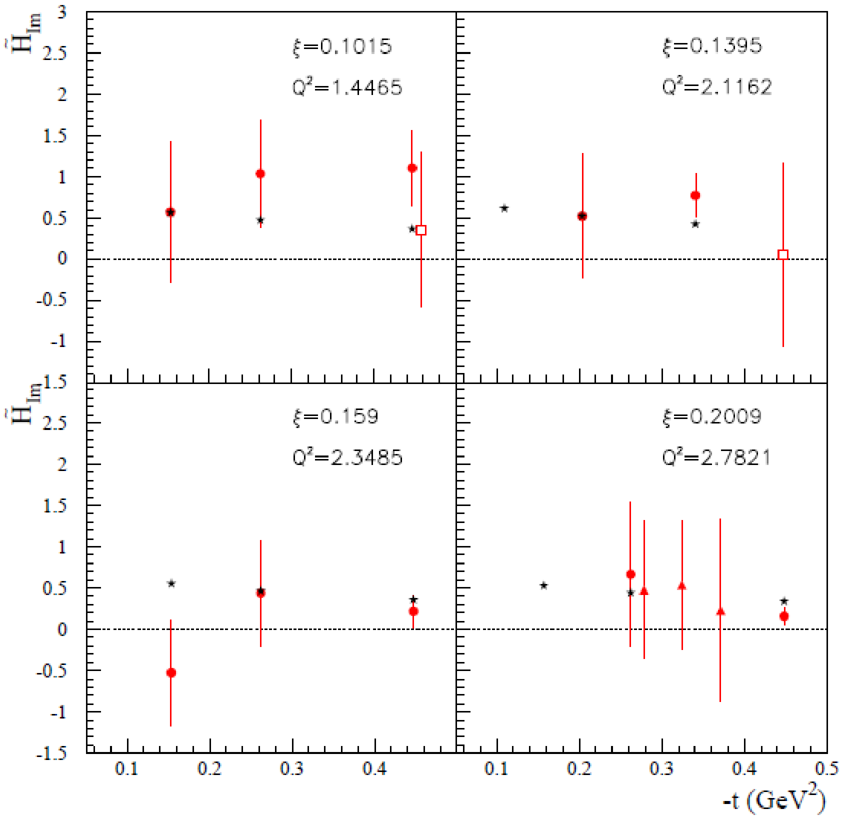

***Im$\mathcal{H}$*, steeper t-slope than *Im$\tilde{\mathcal{H}}$*: the axial charge is more "concentrated" than the electric charge**

Summary of proton-DVCS spin observables and GPDs extraction

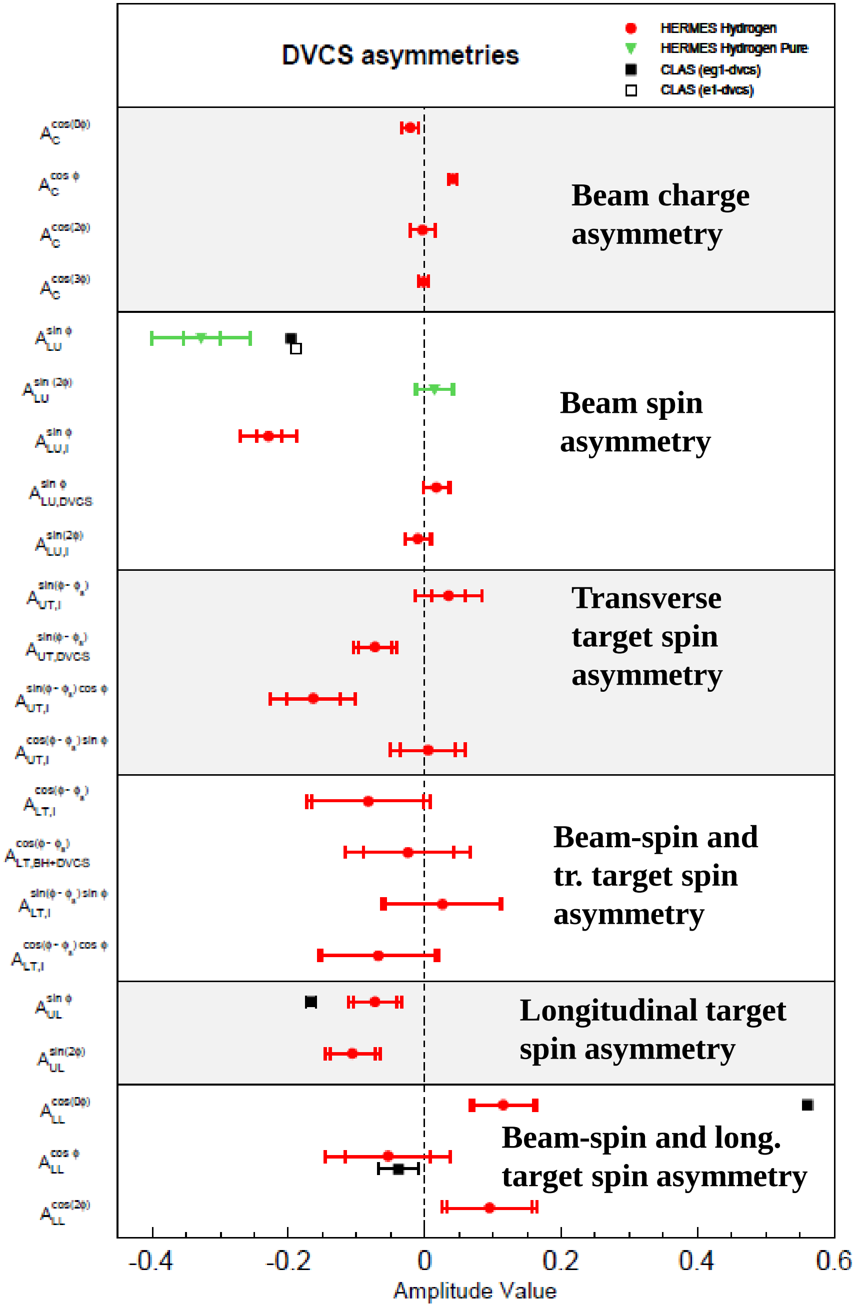

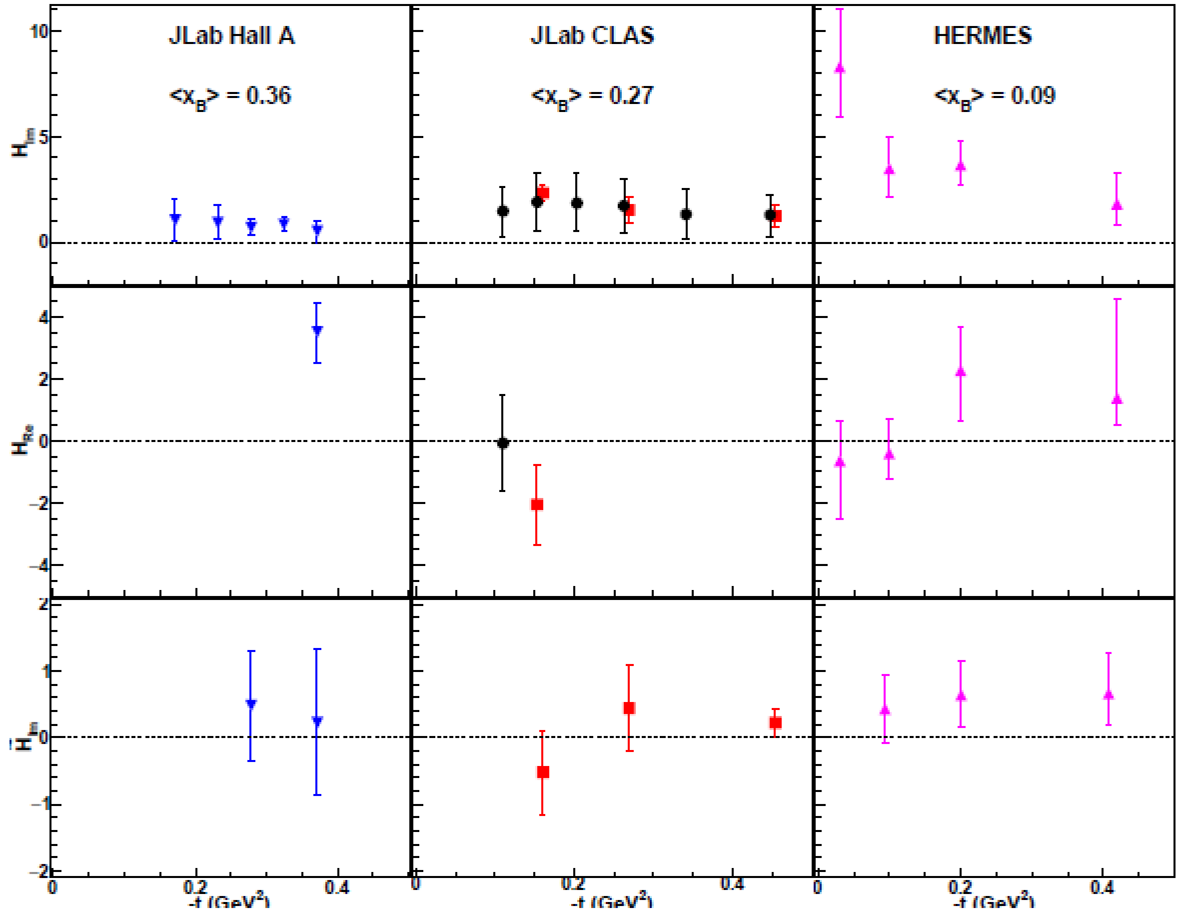

Hall A (2015)

CLAS C.S.

CLAS C.S. +TSA+DSA

HERMES

BCA: strong constraint on H_{re}
→ Motivation for positron beam at JLab

N. d'Hose, S.N., A. Rostomyan, EPJA 52 (2016)

Visualization of proton tomography

Proton tomography obtained from *local fits* to HERMES, CLAS, and Hall-A data (Im$\mathcal{H}$ + model dependent assumptions for x dependence)

High-momentum quarks (valence) are at the core of the nucleon, low-momentum quarks (sea) are at its periphery

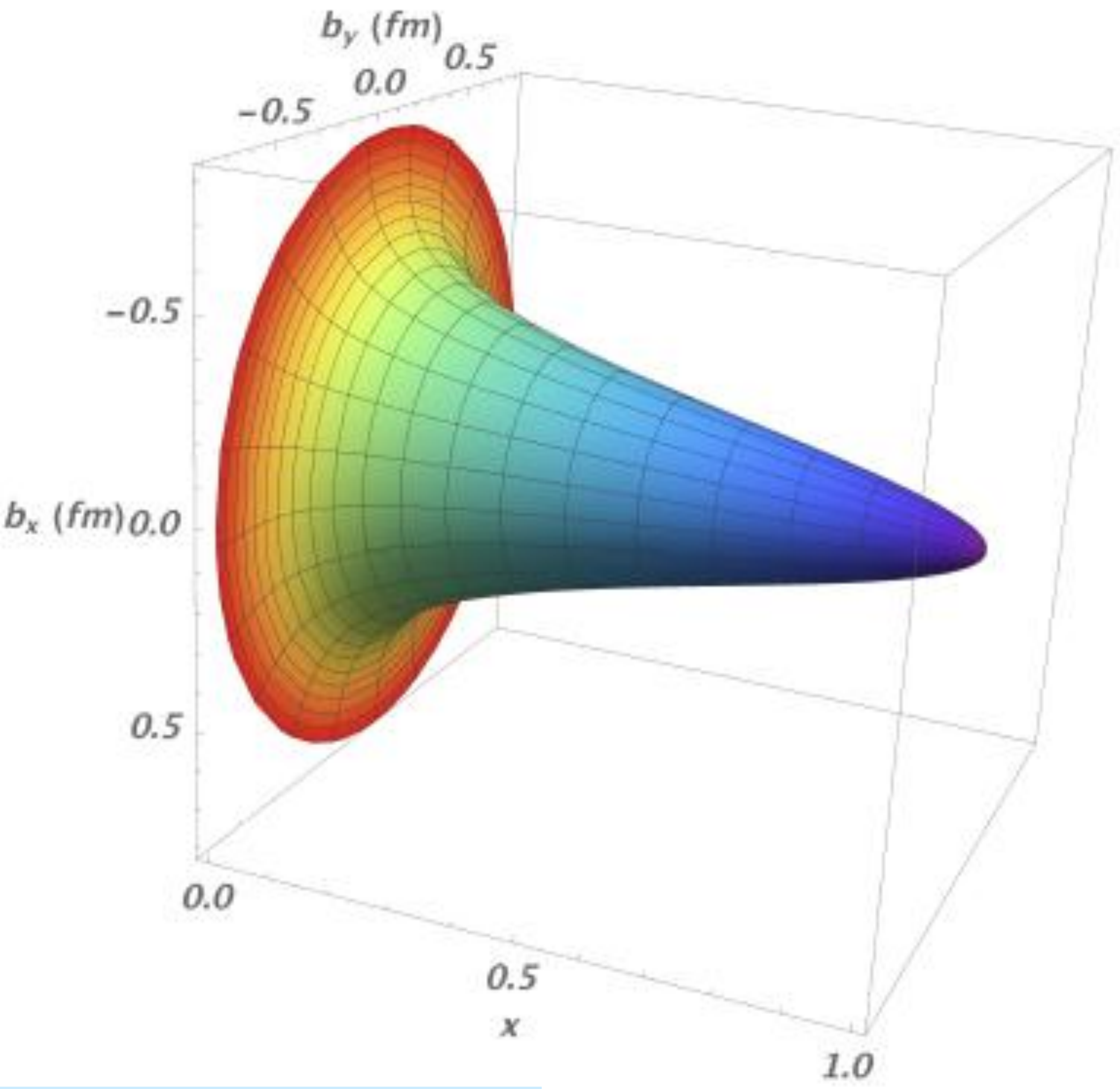

R. Dupré, M. Guidal, M.Vanderhaeghen, PRD95 (2017)

« Visualizing the proton » (R. Milner, R. Ent, R. Yoshida)

Filmmaking by Chris Boebel, Joe McMaster, and James LaPlante

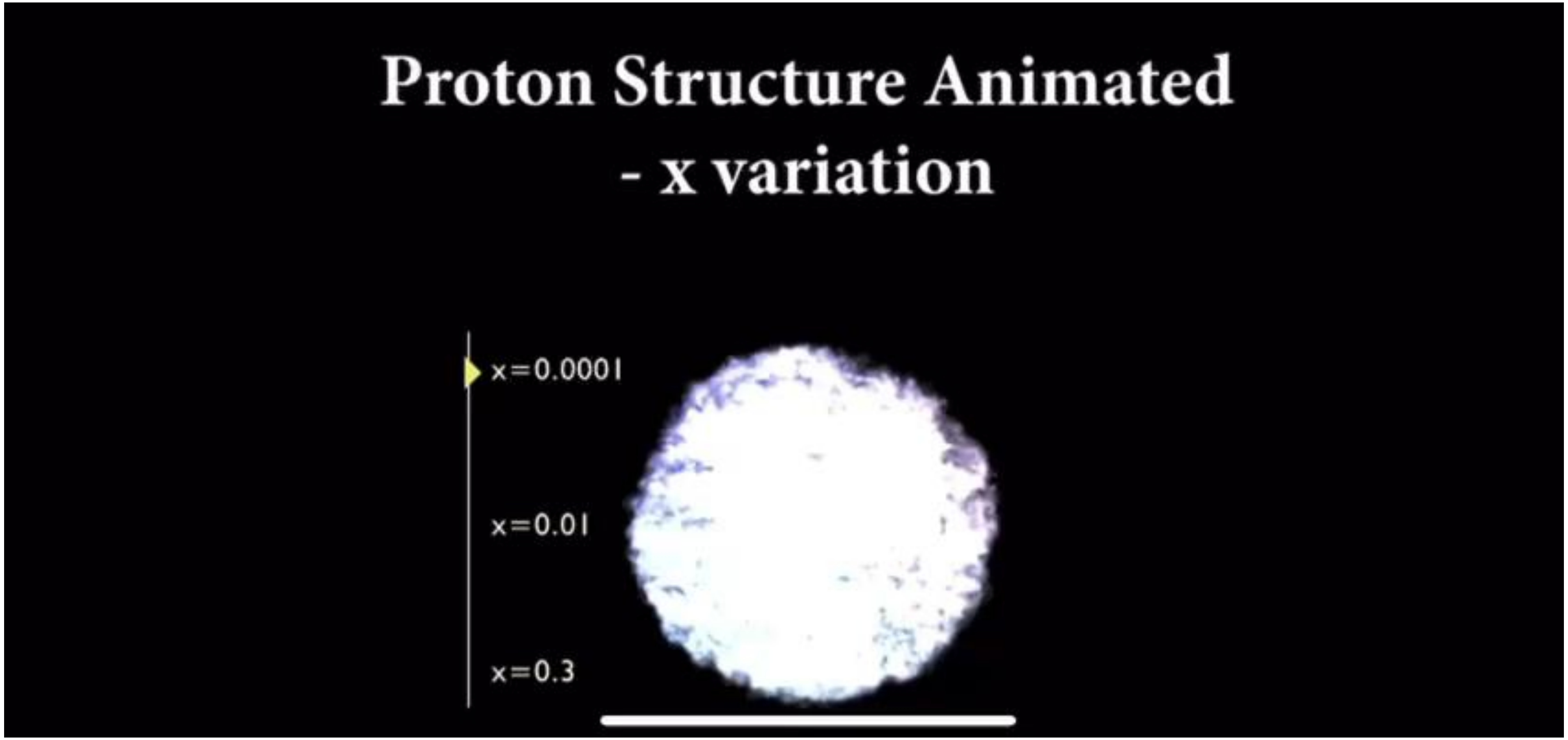

https://www.youtube.com/watch?v=G-9I0buDi4s (published on April 13, 2022)

Distribution of forces in the proton

$$\int xH(x,\xi,t)dx = M_2(t) + \frac{4}{5}\xi^2 d_1(t)$$

Second Mellin moment of H in x: **gravitational form factor** of the energy-momentum tensor → shear forces and pressure (d_1)

$$\mathrm{Re}\mathcal{H}(\xi,t)+i\mathrm{Im}\mathcal{H}(\xi,t)=\int_{-1}^{1}\mathrm{d}x\left(\frac{1}{\xi-x-i\epsilon}-\frac{1}{\xi+x-i\epsilon}\right)H(x,\xi,t)$$

$$\mathrm{Re}\mathcal{H}(\xi,t)\overset{\mathrm{lo}}{=}D(t)+\mathcal{P}\int_{-1}^{1}\mathrm{d}x\left(\frac{1}{\xi-x}-\frac{1}{\xi+x}\right)\mathrm{Im}\mathcal{H}(x,t)$$

Dispersion relation

$$D(t)=\frac{1}{2}\int_{-1}^{1}\frac{D(z,t)}{1-z}\mathrm{d}z \qquad D(z,t)=(1-z^2)[d_1(t)C_1^{3/2}(z)+\cdots]$$

$d_1(t)$ is the first coefficient in the Gegenbauer expansion of the D-term

$$d_1(t)\propto\int\frac{j_0(r\sqrt{-t})}{2t}p(r)\mathrm{d}^3r$$

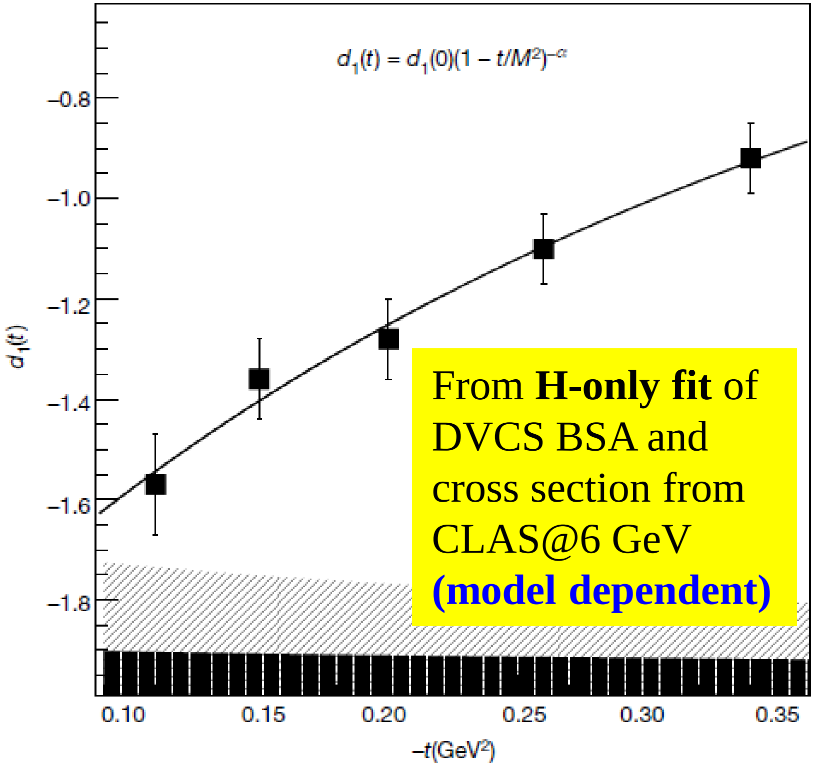

From **H-only fit** of DVCS BSA and cross section from CLAS@6 GeV **(model dependent)**

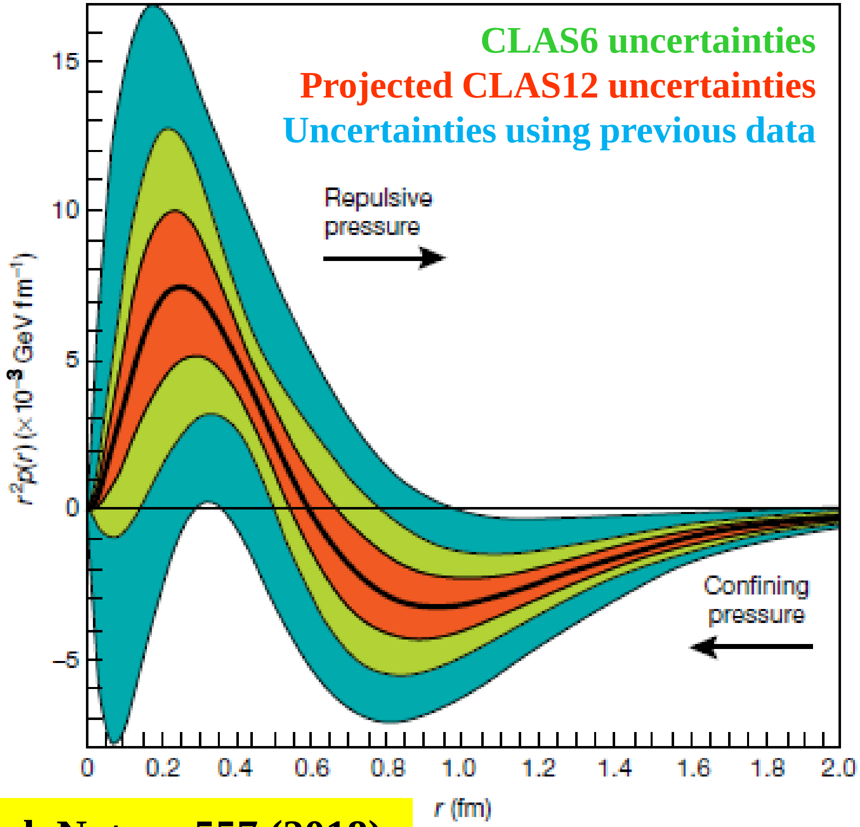

V. Burkert, L. Elouadrhiri, F.X. Girod, Nature 557 (2018)

High-precision DVCS: JLab Hall A at 6 GeV

$\vec{e}p \rightarrow e\gamma(p)$

High precision DVCS cross sections from Hall A (E07-007):
sensitivity to **higher twist** (HT) or **LT-NLO** contributions (gluon exchange)

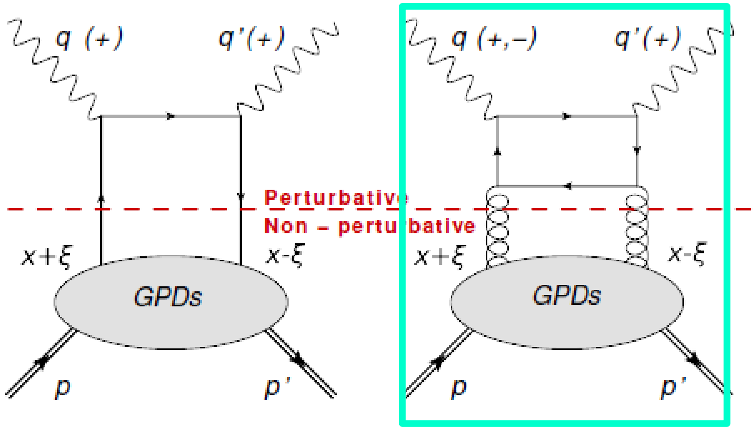

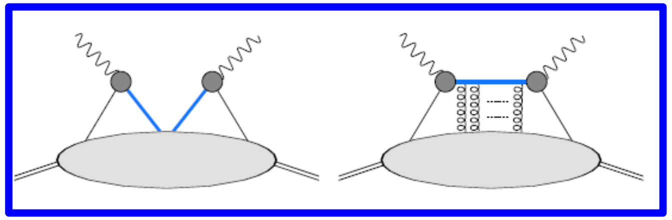

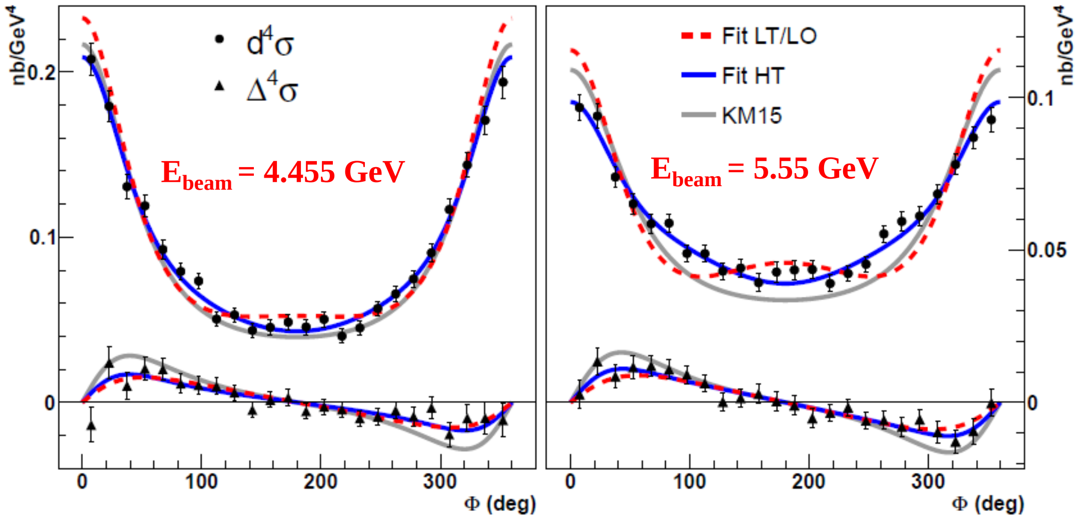

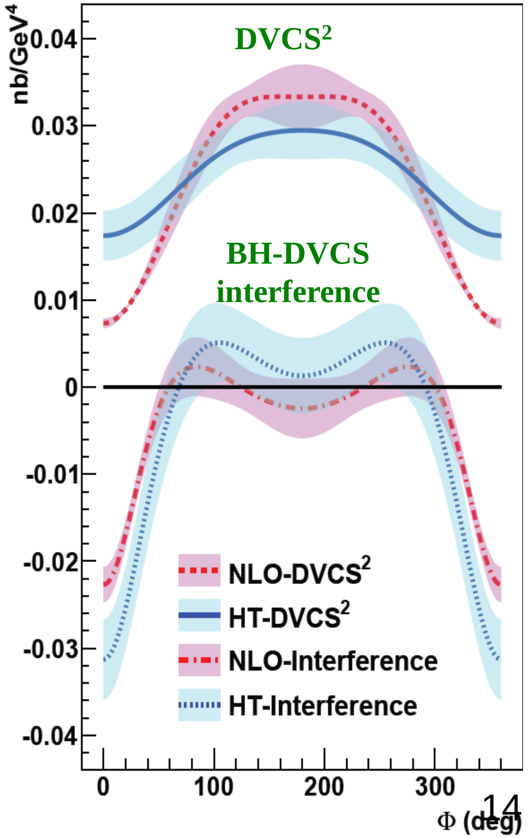

Different beam energies used to separate **BH-DVCS interference ($\sim E_b^3$)** and **DVCS^2 ($\sim E_b^2$)** contributions

M. Defurne *et al.*, Nature Communications 8 (2017)

Interest of DVCS on the neutron

A combined analysis of DVCS observables for proton and neutron targets is necessary for flavor separation of GPDs

$$(H,E)_u(\xi,\xi,t) = \tfrac{9}{15}\left[4(H,E)_p(\xi,\xi,t) - (H,E)_n(\xi,\xi,t)\right]$$

$$(H,E)_d(\xi,\xi,t) = \tfrac{9}{15}\left[4(H,E)_n(\xi,\xi,t) - (H,E)_p(\xi,\xi,t)\right]$$

Moreover, the beam-spin asymmetry for nDVCS is
the most sensitive observable to the GPD E
→ Ji's sum rule for Quarks Angular Momentum

$$\boxed{\frac{1}{2}\int_{-1}^{1} x dx (H^q(x,\xi,t=0) + E^q(x,\xi,t=0)) = J^q}$$

Polarized beam, unpolarized target:

$$\Delta\sigma_{LU} \sim \sin\phi \,\mathrm{Im}\{F_1\mathcal{H} + \xi(F_1+F_2)\tilde{\mathcal{H}} + kF_2\mathcal{E}\}d\phi \quad \Longrightarrow \quad \mathrm{Im}\{\mathcal{H}_n, \tilde{\mathcal{H}}_n, \mathcal{E}_n\}$$

Neutron

Unpolarized beam, transversely polarized target:

Proton

$$\Delta\sigma_{UT} \sim \cos\phi \,\mathrm{Im}\{k(F_2\mathcal{H} - F_1\mathcal{E}) + \ldots\}d\phi \quad \Longrightarrow \quad \mathrm{Im}\{\mathcal{H}_p, \mathcal{E}_p\}$$

The BSA for nDVCS:

- is complementary to the TSA for pDVCS on transverse target, aiming at *E*
- depends strongly on the kinematics → wide coverage needed
- is smaller than for pDVCS → more beam time needed to achieve reasonable statistics

$\vec{e}d \rightarrow e\gamma(np)$

DVCS on the neutron in Hall A at 6 GeV

$$D(e,e'\gamma)X - H(e,e'\gamma)X = n(e,e'\gamma)n + d(e,e'\gamma)d + \ldots$$

Q^2=1.9 GeV^2 x_B=0.36

$$\Delta\sigma_{LU} \sim \sin\phi \; \mathrm{Im}\{F_1\mathcal{H} + \xi(F_1+F_2)\widetilde{\mathcal{H}} - kF_2\mathcal{E}\}$$

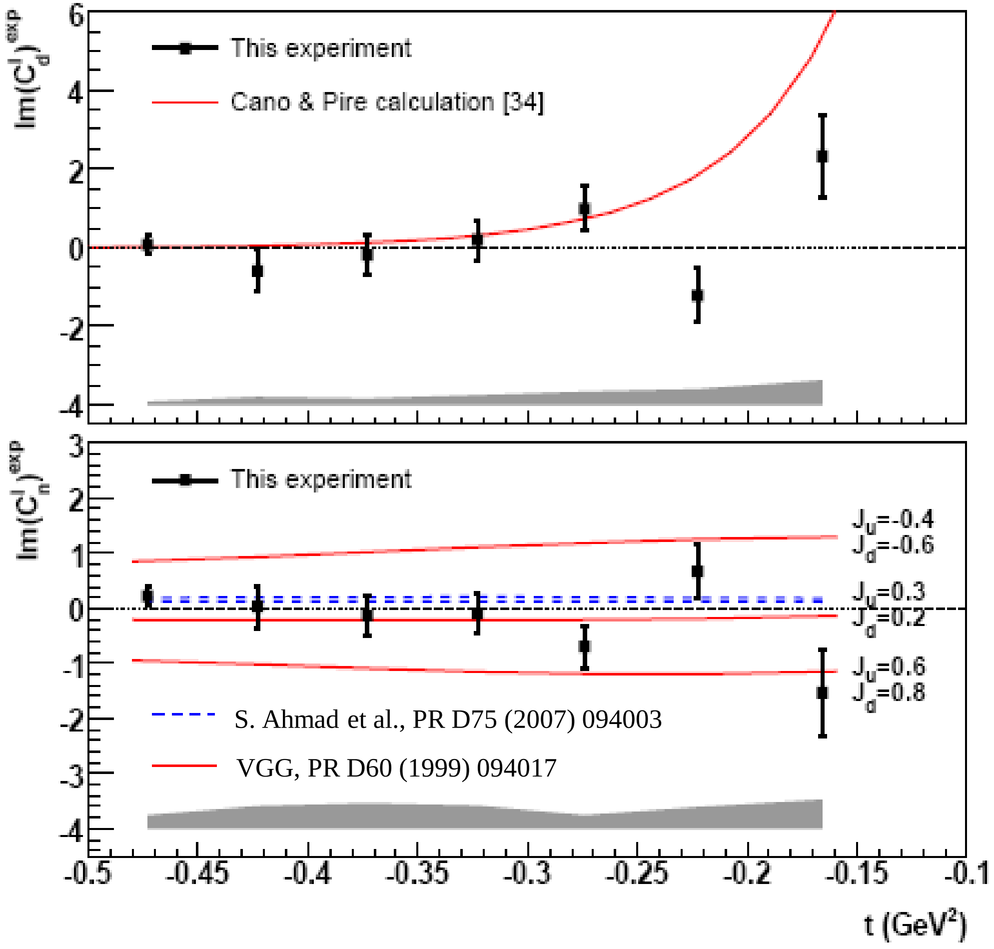

M. Mazouz et al., PRL 99 (2007)

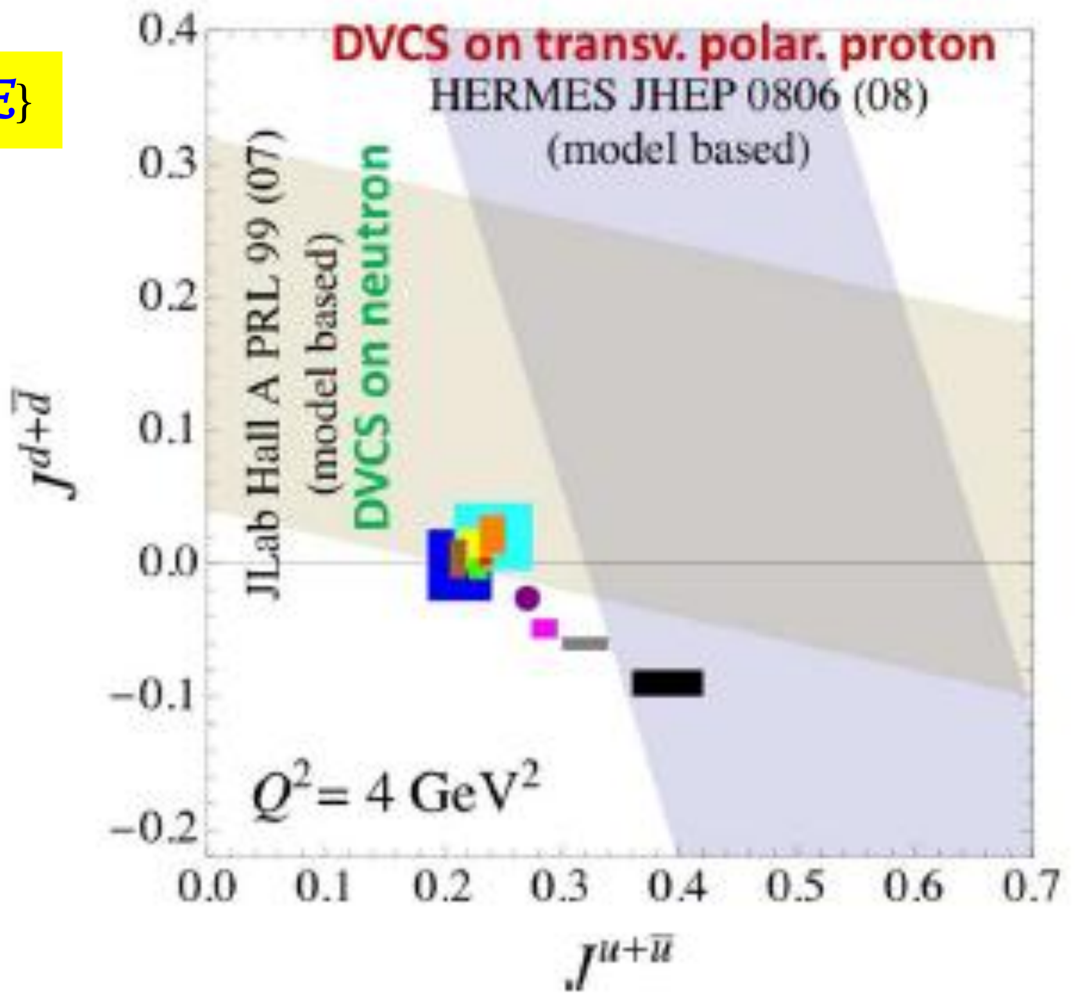

- **E03-106: First-time measurement of $\Delta\sigma_{LU}$ for nDVCS**
- **Model-dependent extraction of J_u, J_d**

$\vec{e}d \rightarrow e\gamma(np)$

DVCS on the neutron in Hall A at 6 GeV

$$D(e,e'\gamma)X - H(e,e'\gamma)X = n(e,e'\gamma)n + d(e,e'\gamma)d + \ldots$$

Q^2=1.9 GeV^2 x_B=0.36

nDVCS and coherent **dDVCS** separated through MM^2_X shift:

- large correlations at low –t
- good separation at larger -t

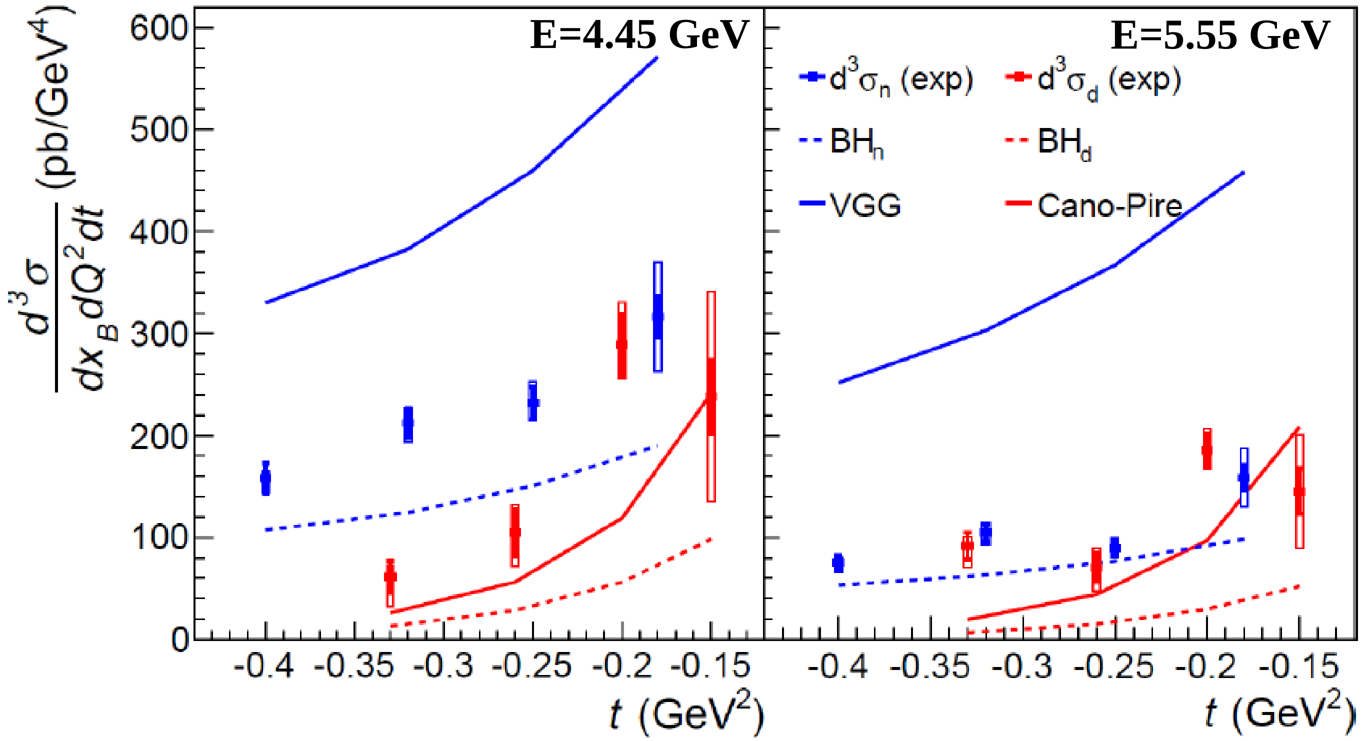

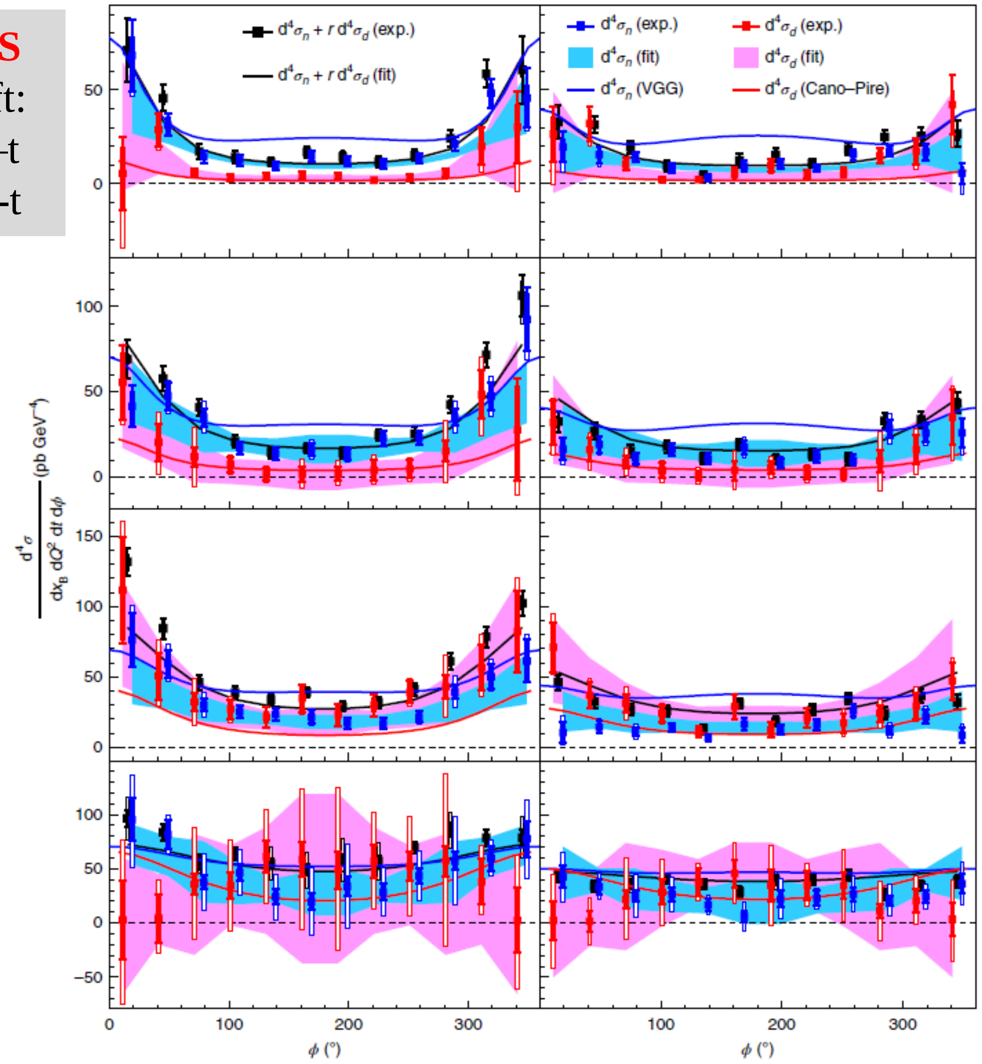

E=4.45 GeV **E=5.55 GeV**

Hall-A experiment E08-025 (2010)

- Beam-energy « Rosenbluth » separation of nDVCS CS (two beam energies)
- First observation of non-zero nDVCS CS
- **M. Benali et al., Nature 16 (2020)**

Summary

- DVCS is the reaction more directly interpretable in terms of GPDs
- The interference of DVCS with Bethe Heitler depends linearly on the Compton Form Factors (linked to GPDs) and can be accessed experimentally measuring spin asymmetries
- CLAS and HERMES provided the first observation of DVCS-BH interference
- Since then, a wealth of dedicated experiments were carried out, in particular at JLab@6 GeV (Halls A and B):
    - BSA, TSA, DSA for pDVCS
    - Cross sections for pDVCS, high precision (Hall A) and wide coverage (CLAS)

    → first tomographic image of the proton

    → first glance at the pressure distribution in the proton
    - First measurements of DVCS on the neutron (Hall A):

    → First model-dependent extraction of J_u, J_d

    → First observation of non-zero cross section for nDVCS